(NASA-CR-169638) AN EXPERIMENTAL INVESTIGATION OF INTERNAL AREA RULING FOR TRANSONIC AND SUPERSONIC CHANNEL FLOW Final Scientific Report, 25 Sep. 1981 - 24 Sep. 1982 (San Jose State Univ., Calif.) 99 p G3/02

N83-14068

Unclas 02182

SAN JOSE STATE UNIVERSITY
DEPARTMENT OF MECHANICAL ENGINEERING

AN EXPERIMENTAL INVESTIGATION OF INTERNAL AREA RULING FOR TRANSONIC AND SUPERSONIC CHANNEL FLOW

By

William B. Roberts
Research Associate
Department of Mechanical Engineering
San Jose State University, San Jose, CA
and
Flow Application Research, Fremont, CA

Harry L. van Rintel
Graduate Student
Department of Mechanical Engineering
San Jose State University, San Jose, CA
and
Senior Engineer
Lockheed Missiles and Space Co., Sunnyvale, CA

and

Ghaus Rizvi
Graduate Assistant
Department of Mechanical Engineering
San Jose State University, San Jose, CA

August 24, 1982

Final Scientific Report on Grant NAG 3-196
to NASA-Lewis Research Center, Fan and Compressor Branch,
Cleveland, Ohio

SAN JOSE STATE UNIVERSITY
DEPARTMENT OF MECHANICAL ENGINEERING

AN EXPERIMENTAL INVESTIGATION OF INTERNAL AREA RULING FOR TRANSONIC AND SUPERSONIC CHANNEL FLOW

By

William B. Roberts
Research Associate
Department of Mechanical Engineering
San Jose State University, San Jose, CA
and
Flow Application Research, Fremont, CA

Harry L. van Rintel
Graduate Student
Department of Mechanical Engineering
San Jose State University, San Jose, CA
and
Senior Engineer
Lockheed Missiles and Space Co., Sunnyvale, CA

and

Ghaus Rizvi
Graduate Assistant
Department of Mechanical Engineering
San Jose State University, San Jose, CA

August 24, 1982

Final Scientific Report on Grant NAG 3-196
to NASA-Lewis Research Center, Fan and Compressor Branch,
Cleveland, Ohio

ABSTRACT

The prediction of aerodynamic performance of part-span dampers for transonic rotors has been reported in literature from the National Aeronautics and Space Administration [1, 2, 3, 4][1]. Part-span dampers are necessary on the high aspect ratio transonic fans used in modern aircraft fan-jet engines. The use of part-span dampers requires that their drag effects on the flow through the rotor blade passages be minimized. It may be possible to do this by incorporating an internal area rule.

The purpose of this investigation was to examine a simulated transonic rotor channel model experimentally at San Jose State University to verify the flow physics of internal area ruling. Pressure measurements were performed in the high speed wind tunnel at transonic speeds with Mach 1.5 and Mach 2 nozzle blocks to get an indication of the approximate shock losses.

The results showed a reduction in losses due to internal area ruling with the Mach 1.5 nozzle blocks. The reduction in total loss coefficient was of the order of 17 percent for a high blockage model and 7 percent for a cut-down model.

---

[1]Numbers in brackets are references located at the end of this Report.

TABLE OF CONTENTS

NOMENCLATURE

A	geometric area
A*	critical area
AR	area ruled
c	chord
L	nozzle block length
M	Mach number
mm	millimeter
NB_s	nozzle blocks
P	pressure
P_b	barometric pressure
P_o	stagnation pressure
P_{o1}	average stagnation pressure in settling chamber
P_{o2}	average stagnation pressure downstream of model
P_s	static pressure
PSD	part-span damper
psi	pressure (pounds per square inch)
psia	absolute pressure (pounds per square inch)
$\bar{\omega}_c$	channel total pressure loss coefficient
t	thickness
V	volt
x	distance from test section center in direction of flow
y	vertical distance from test section center, positive upward

AN EXPERIMENTAL INVESTIGATION OF INTERNAL AREA RULING FOR TRANSONIC AND SUPERSONIC CHANNEL FLOW

1. INTRODUCTION

Over the past several years, considerable effort has been devoted to the improvement of jet engines because of a national interest in fuel efficient aircraft. Such attempts require major revisions in each sub-unit along with improvements of every component of the engine. For example, one area for significantly increasing the performance of a turbofan engine lies in improving the compressor by a redesign of the blades. The use of high-aspect-ratio blades (blades with a high ratio of blade span to blade chord) is a method to decrease the engine weight, while maintaining the pressure producing capability. To assure stability and a rigid structure, these high-aspect-ratio blades are bridged together by a shroud called "part-span dampers" (Fig. 1). Unfortunately, these part-span dampers (PSDs) induce a loss in the aerodynamic performance of a rotor stage by creating additional shock and wake losses, and they also influence the region directly behind the damper causing adverse flows for the stator blades [1, 2, 3, 4].

Experimental studies using rotor blading with PSDs have been conducted at the NASA/Lewis Research Center, sponsor of this project. Roberts (4) described a series of actions that could lead to increased efficiency for turbofan engines using area ruling concepts. The idea is to reshape the narrow

channels caused by adjacent blades and the PSD by applying an internal area ruling. Several blade designs using PSDs conforming to basic airfoil shapes have been proposed by Roberts. However, no significant relations from the standpoint of optimum size and shape have yet been determined, primarily because of unresolved questions concerning the nature of the three-dimensional transonic flow in the rotor section. Because of these questions, and the fact that present theoretical or numerical methods are incapable of solving complicated fluid flows, simplified tests are necessary to analyze the various proposed configurations.

The purpose of this investigation was to produce and test a transonic straight channel model representing an uncambered cascade of double wedge airfoils with an angle-of-attack of zero degrees (Fig. 2). The area rule will be applied to this model by removing material from the side wall (Figs. 3 and 4).

The model was developed to fit the six by six inch test section of the San Jose State University (SJSU) high speed wind tunnel. Static and impact pressure measurements in the areas of immediate interest were conducted at transonic speeds to obtain the loss coefficients of the channel model with the Mach 1.5 and 2 nozzle blocks.

2. MODEL APPARATUS

Experimental Model

The model used in this experiment was designed by the authors from sketches shown in Reference 4. A double-wedge

profile was suggested with the blade thickness ratio (t/c) of 10 percent, and the part-span damper thickness ratio (t/c) about 30 percent. The symmetrical parts were fabricated from type 303 stainless steel by the SJSU experimental shop. To support the blade assembly rigidly in the center of the test section, the glass windows had to be replaced by solid side walls. These were machined from 6061-T6 aluminum. The use of a relatively soft material for these plates would allow ease of machining for the area ruling experiment. The dimensions of the blade and PSD were made as large as possible for ease of manufacturing, and to prevent structural failure. Conservative stress calculations revealed an approximate shear load of 149 pounds with maximum bending stresses of 3900 psi on the PSD, and respectively about 150 pounds and 600 psi on the blade, assuming a wind-tunnel dynamic pressure of 100 psi. The material yield strength in an annealed condition was listed as 30000 psi. The ultimate shear load of the 1/4-28 bolts was 3600 pounds. To minimize flow disturbances, all slots and cavities were sealed with filler compound.

Earlier, smaller blade and PSD dimensions were studied including the use of half blades, different materials, and a vertical blade position. The test model was eventually designed with special attention to manufacturing cost and safety (Fig. 3). Copies of the model drawings are shown in Appendix A. The area ruled configuration is shown in Fig. 4,

where a half wedge of material has been removed from each side wall to compensate for the damper.

Supersonic Wind Tunnel

The investigation was conducted in the six by six inch supersonic blowdown-type wind tunnel built by Kenney Engineering Corporation and located at the San Jose State University Mechanical Engineering Laboratory. It is shown in Fig. 5. The test section Mach number can be varied between 1.5, 2, 3 and 4.5 by insertion of the appropriate interchangeable fixed nozzle blocks. In this case, the Mach 1.5 and 2 nozzle blocks were used. The original design of these blocks was done by the method of characteristics and includes boundary layer effects at a median Reynolds number to produce a consistent Mach number in the test section (5, 6 and 7). The wind tunnel was also equipped with a variable area second throat to form a supersonic diffuser. Static pressure taps were drilled in both the Mach 1.5 and 2 blocks just upstream from the model to enable the detection of possible shocks and to verify flow symmetry. The number of #80 holes was limited since the scanning valve contained only 48 pressure connections. Because of the model position in the center of the test section, interference was encountered with the existing rake. A new shorter 9-probe rake was designed and manufactured (Fig. 6). Also, a shorter sting holder was installed to move the new rake farther back in the test section. A

more complete description of this wind tunnel and its operation is found in References 8 and 9.

Instrumentation and Control

The high speed wind tunnel instrumentation consisted of two quartz piezolectric pressure transducers for measuring the pressures in the tunnel and test section. Plenum, nozzle blocks, test section, rake and diffuser pressures were measured consecutively using a Scanivalve Model J-48 containing one of the pressure transducers coupled to a Sanborn 2-channel chart recorder via a charge amplifier. To record the tunnel average pressures in the settling chamber, the other pressure transducer sensing four pressure taps was connected to a second charge amplifier and linked to the Sanborn recorder. Ambient pressures were read separately on a standard laboratory mercury barometer. The tunnel has an electrically-driven traverse mechanism which allowed the sting holder to be moved vertically to any desired position. A pneumatic controller and valve positioner with a six-inch throttle plug (Fig. 7) controlled the stagnation pressure of the wind tunnel. The controller is equipped with proportional band and reset controls. It is controlled from a panel which has the appropriate switches for starting and stopping the tunnel. The traverse mechanism is also operated from this control panel. The wind tunnel also has an air drier to prevent condensation shock waves. A more detailed description can be seen in Reference 8.

Calibration

Prior to operating the wind tunnel, the two quartz piezoelectric transducers were calibrated. For the one used on the settling chamber, hydraulic pressure was applied by means of a deadweight tester. The output, converted by a charge amplifier, was then read onto the Sanborn recorder. This circumvented individual component/instrument errors. A standard error analysis of this system indicated calibration inaccuracies of 0.18 psi when a least square fit was used to obtain a conversion formula. The transducer contained in the scanning valve, engaged to a second amplifier, was connected to the shop air supply through a pressure regulator and gauged against a mercury manometer and the output recorded on the Sanborn recorder. This allowed calibration in the negative pressure range. The standard deviation of these readings deduced from a least square fit was 0.13 psi.

The Sanborn dual channel recorder was tested for proper deflection on each day of use with the aid of a C-size battery. The battery voltage was first checked with a digital voltmeter.

Difficulties were encountered in obtaining a constant upstream stagnation pressure. However, this is not necessary since all the downstream stagnation pressures correlate with the upstream stagnation pressures. Although there was some initial fluctuation in tunnel stagnation pressure at the start of a run, the flow finally stabilized sufficiently

to yield reliable data. A stable run time of about 6 seconds was necessary to complete the 48-port scan.

The wind tunnel itself was calibrated as follows: First the stagnation pressure was checked to see if the indicated control pressure correlated with the stagnation chamber transducer readings. Then, with the Mach 1.5 nozzle blocks, a half-inch diameter cone with a half angle of 7° (Fig. 8) was used to evaluate the Mach number in the test section. The half-inch diameter cone produced an attached shock wave with angle of 43°, which indicated a Mach number of 1.47 (see Fig. 8). An attempt to put a larger frontal area wedge or cone in the test section failed to produce an attached shock because of excess blockage. The reason for this was that the 20° wedge, with a frontal area of 4.77 square inches and blockage ratio of 13.26 percent, formed an area ratio $A/A^* = 1.049$, which was just above the value required for sonic conditions in isentropic flow (i.e., $A/A^* = 1$). The 3-inch diameter cone (half angle 20°) which has approximately the same area blockage as the blade/PSD model, produced no signs of supersonic flow regardless of higher stagnation pressure input. This cone had a frontal area of 7.07 square inches and a blockage ratio of 19.64 percent.

Calibration data is shown in Appendix C.

3. PROCEDURE

Pressure Measurements with Mach 1.5 Nozzle Blocks

Initially, a series of runs were made at several stagnation pressure settings to verify the structural integrity of the test model and rake, to check for possible discrepancies in the readouts, leaks in the tube connections, and to determine stable flow settings. Control settings of about 12 psi stagnation pressure were selected for the subsonic tests with a closed diffuser position of 1-5/8 inches on each side, leaving a second throat area of 6 by 2-3/4 inches. For the transonic tests, the stagnation pressure setting was slightly increased and the diffuser was opened fully. These settings gave a stable flow after an initial fluctuation period of approximately two seconds. Runs were made to generate the data for evaluating the model viscous and shock losses. The rake was positioned vertically at half-inch intervals, requiring 11 runs to traverse the six-inch test section height. Several redundant runs were made to verify consistency and to determine the repeatability of measurements.

Tests were made for subsonic and transonic flow, with and without area ruling. A few representative samples of the pressures measured at the tunnel side wall and test section side plate are shown in Figs. 9, 10 and 11. The subsonic run shows a relatively low pressure variation, indicating subsonic flow everywhere.

The transonic runs show a larger variation. They start with a steady drop in pressure (nearly reaching sonic flow), then there is a rise in pressure after the throat (subsonic flow, due to model blockage) and a re-expansion of the flow through the model to supersonic speed, and finally shock down indicated by the cusp. This is caused by the shape of the model forming a converging-diverging nozzle.

It was found that, for the subsonic runs, the upstream static pressure was lower than at some of the downstream ports. This phenomena was attributed to the fact that the tunnel was designed for supersonic flows. For subsonic flow, the area increase downstream of the throat acts as a diffuser, which significantly increases the static pressure in the end-wall regions. To measure the pressure in the flow properly, a total pressure probe was inserted upstream of the test model (X = 1 inch), as shown on Fig. 12. Also, pressure taps were added in the model side wall plate to detect shock waves generated by the model.

Pressure Measurements with Mach 2 Nozzle Blocks

The procedures used for these runs were essentially the same as for the Mach 1.5 nozzle blocks, except with higher input stagnation pressure settings for the supersonic runs. Pressure distributions of a few selected runs shown in Figs. 13 and 14 are again nearly identical for the straight and area ruled channel configuration. They also indicate that an

oblique shock stands approximately 10 inches upstream of the model, where the flow is supersonic. If blockage due to the model size was not so great, the line would have followed a decreasing pressure path.

Subsonic flow with these nozzle blocks would show a pressure line similar to that with the Mach 1.5 blocks, as in Fig. 9.

4. INITIAL RESULTS

Typical results of the rake pressure measurements are shown in Figs. 15 to 20. They are plotted from the tabulated data in Appendix C. A few samples of the actual recorder strips from which these data and plots are derived are also included in Appendix C.

The average stagnation pressure (P_{o1}) for all the plots is 27.00 psia, except for the two sets of runs with the Mach 2 nozzle blocks, which are 40.50 psia. The area averaged rake stagnation pressures (P_{o2}), downstream of the model, are

For M-1.5 Nozzle Blocks (NB_s)

$M_1 = 0.43$, P_{o2} (subsonic) = 26.46 psia

$M_1 = 0.63$, P_{o2} (transonic) = 23.56 psia

$M_1 = 0.63$, P_{o2} (transonic,AR) = 24.16 psia

where AR denotes area ruling and M_1 is the Mach number immediately ahead of the model.

For M-2 Nozzle Blocks (NB_s)

$M_1 = 0.49$, P_{o2} (subsonic) = 25.62 psia

$M_1 = 1.07$, P_{o2} (supersonic) = 27.15 psia

$M_1 = 1.11$, P_{o2} (supersonic,AR) = 27.22 psia

From the above, the pressure losses

$\Delta P_o = P_{o1} - P_{o2}$ are calculated

For M-1.5 NB_s

ΔP_o (subsonic) = 27.00 - 26.46 = 0.54 psia

ΔP_o (transonic) = 27.00 - 23.56 = 3.44 psia

ΔP_o (transonic,AR) = 27.00 - 24.16 = 2.84 psia

For M-2 NB_s

ΔP_o (subsonic) = 27.00 - 25.62 = 1.38 psia

ΔP_o (supersonic) = 40.50 - 27.15 = 13.35 psia

ΔP_o (supersonic,AR) = 40.50 - 27.22 = 13.28 psia

The total pressure loss coefficient for the channel is defined as

$$\bar{\omega}_c = (P_{o1} - P_{o2})/P_{o1}$$

For M-1.5 NB_s

$\bar{\omega}_c$(viscous) = $(P_{o1}-P_{o2})/P_{o1} = \Delta P_o/P_{o1}$ = 0.54/27.00 = 0.020

$\bar{\omega}_c$(transonic) = $\Delta P_o/P_{o1}$ = 3.44/27.00 = 0.127

$\bar{\omega}_c$(transonic,AR) = $\Delta P_o/P_{o1}$ = 2.84/27.00 = 0.105

Note: Viscous loss coefficient obtained from subsonic pressures.

For M-2 NB_s

$\bar{\omega}_c$(viscous) $= \Delta P_o/P_{o1} = 1.38 / 27.00 = 0.051$

$\bar{\omega}_c$(supersonic) $= \Delta P_o/P_{o1} = 13.5 / 40.50 = 0.330$

$\bar{\omega}_c$(supersonic,AR) $= \Delta P_o/P_{o1} = 13.28 / 40.50 = 0.328$

Normally, for transonic and supersonic flow, the shock loss coefficients are obtained by subtracting the viscous loss coefficient from the total loss coefficients. However, because the viscous loss coefficients for runs with M-1.5 and M-2 nozzle blocks fell within the repeatability range of 5%, it was omitted and thus the value and reduction in SHOCK LOSS could not be determined. The reduction in TOTAL LOSSES due to area ruling is

For M-1.5 NB_s

$$\text{Percent Reduction}_{(M-1.5)} = \frac{\bar{\omega}_{c(\text{transonic})} - \bar{\omega}_{c(\text{transonic,AR})}}{\bar{\omega}_{c(\text{transonic})}} \times 100\%$$

$$= \frac{0.127 - 0.105}{0.127} \times 100\%$$

$$= 17.32\%$$

This is greater than the error band of $\pm$5%, and is therefore considered significant.

For M-2 NB_s

$$\text{Percent Reduction}_{(M-2)} = \frac{\bar{\omega}_{c(\text{supersonic})} - \bar{\omega}_{c(\text{supersonic,AR})}}{\bar{\omega}_{c(\text{supersonic})}} \times 100\%$$

$$= \frac{0.330 - 0.328}{0.330} \times 100\%$$

$$= 0.61\%$$

This is well within the repeatability range and, therefore, is not significant.

Figures 21 through 26 show test section Mach number distribution for comparison. These Mach numbers were obtained from the static pressure taps in the side wall plate shown in Fig. 12.

5. MODIFIED MODEL

Due to the relatively large frontal area of the original channel test model, the tunnel did not start (i.e., operate at or near the design Mach number in the test section). During the last phase of testing, an effort was made to alleviate this condition by cutting down the double wedge model to a "double trapezoid" model, as is shown in Figure 27. This figure shows a cut-down central blade and damper with a blockage ratio of 10.3%, compared to 18.25% for the original model (i.e., blockage ratio = $A_{model}/A_{test\ sect.}$ X 100%).

This model was tested with the Mach 1.5 and 2.0 nozzle blocks, with and without area ruling. Two forms of area ruling were used: (1) area ruling to compensate for the damper, Figure 28, and (2) area ruling to compensate for the damper and central blade, Figure 29. The latter was done to determine if there would be any effect of having an area distribution through the test section of near "zero" blockage. Drawings of the modified model are shown in Appendix A.

6. MODIFIED MODEL RESULTS

The same measurements were taken with the modified model as for the original, with the exception that part of the data was reduced "on line" by an Apple Computer System. Difficulties with the system resulted in the loss of some data, namely that pressure data which allowed the calculation of the Mach number distribution through the test section for the M-1.5 nozzle blocks. However, measurements were available that permitted the calculation of the inlet Mach number. The static pressure distribution for the M = 1.5 and 2.0 nozzle blocks are shown in Figures 30 and 31.

The results of the rake measurements are similar to those given in Figures 15-20, and are listed in Appendix C. In order to have steady tunnel operation, the stagnation pressure setting had to be varied for the different area ruling tests. Therefore, the stagnation chamber pressure (P_{o1}) and the area averaged rake total pressure (P_{o2}) are given for each test series:

For M-1.5 NB_s

Straight Channel - $M_1 = 0.75$, $P_{o1} = 36.5$ psia, $P_{o2} = 32.2$ psia

AR, Damper - $M_1 = 0.79$, $P_{o1} = 36.5$ psia, $P_{o2} = 32.2$ psia

AR, Damper & Blade - $M_1 = 0.9$, $P_{o1} = 31.0$ psia, $P_{o2} = 27.6$ psia

For M-20 NB_s

Straight Channel - $M_1 = 1.99$, $P_{o1} = 33.6$ psia, $P_{o2} = 23.9$ psia

AR, Damper & Blade - $M_1 = 2.0$, $P_{o1} = 38.0$ psia, $P_{o2} = 27.1$ psia

From the above values, the channel total pressure loss coefficient, $\bar{\omega}_c = (P_{o1} = P_{o2})/P_{o1}$, can be calculated:

For M-1.5 NB_s

Straight Channel - $\bar{\omega}_c = 0.118$

AR, Damper - $\bar{\omega}_c = 0.118$

AR, Damper & Blade - $\bar{\omega}_c = 0.110$

For M-2.0 NB_s

Straight Channel - $\bar{\omega}_c = 0.289$

AR, Damper & Blade - $\bar{\omega}_c = 0.287$

For the M-1.5 nozzle blocks, the model with full area ruling (i.e., damper and blade) showed a reduction in loss coefficient of ~6.8%. With the M-2.0 nozzle block, the decrease was ~0.7%. The first is only slightly larger than the range of repeatability and the latter is inconsequential.

7. DISCUSSION

The static pressure distribution for the tests done indicate that, in most cases, the tunnel did not start. This is shown in Figures 9-11 by the subsonic flow up to the model, whereupon the flow chokes at the maximum model area (i.e., minimum tunnel area). Figures 13, 14 and 30 show a sudden increase in static pressure just before the test section, indicating the presence of a normal or oblique shock. The

only high speed tests for which the tunnel started were those for the modified model using the M-2.0 nozzle blocks. For all of the transonic runs, the model blockage was too great to allow the tunnel to start. For two of the tests, the Mach number at the model inlet was slightly supersonic ($M \simeq 1.05$) after the main tunnel shock.

A summary of data showing channel loss coefficient plotted with inlet Mach number is shown in Figure 32. For the original model, there is a 17.2% difference in loss coefficient at $M_1 = 0.63$ (M-1.5 NB_s) and no difference for $M \simeq 1.05$ (M-2.0 NB_s). For the modified model, there was a small drop of 6.8% in loss coefficient for the fully area ruled case (area ruled for both damper and blade) using the M-1.5 NB_s. The main difference in these tests was the model inlet Mach number. Area ruling had the effect of increasing the model inlet Mach number from 0.75 for the straight wall, to 0.9 with full area ruling. This is a significant increase for the transonic range. There was no significant performance difference for the modified model between straight and area ruled cases at $M_1 = 2.0$. However, this is in agreement with Witcomb's (10) findings; that is, at Mach numbers at or above twice the speed of sound, the area rule ceases to have any effect for external flow.

The present experimental results indicate that the effect of area ruling on the shock losses of a simplified internal channel blade and damper model is not great. This

could be due to the excessive blockage caused by the models that precluded tunnel starting, or due to the crude shape of the model and area ruling contours. A model with a lower blockage ratio, that would allow the tunnel to start, might show a greater effect of area ruling. Furthermore, it is known (10, 11) that, as the gradient of area becomes irregular or discontinuous, wave drag increases. The original model has at least one sudden change of slope that a smoothly-curved model would not; that is, the apex of the wedge. The cut-down trapezoid model and damper has an additional three discontinuities (i.e., a total of four). It is possible that a model using a bi-convex blade and damper might show a greater difference between the straight wall and area ruled condition.

8. SUMMARY

Pressure measurements have been taken on blade and damper models, with and without area ruling, in a 6" x 6" high speed blow down wind tunnel. An original double wedge model having 18.3% area blockage ratio was used and subsequently cut down to a double trapezoid with 103% blockage. The tunnel would not start with either model using the transonic nozzle blocks (M = 1.5). The tunnel did start with the cut-down model using the supersonic nozzle blocks (M = 2.0).

A difference of 17.32% in channel pressure loss coefficient was observed between the straight wall and area ruled

double wedge at low transonic speed. A 6.8% decrease in loss coefficient and an increase in inlet Mach number was measured for the double trapezoid model between the straight wall and area ruled cases in the low transonic regime.

There was no significant difference between straight and area ruled model performance for low or high supersonic speeds.

9. ACKNOWLEDGEMENT

The authors would like to acknowledge the administrative assistance of Professor Helmer Nielsen, Chairman, Department of Mechanical Engineering, and the San Jose State University Foundation. The authors are also grateful to Mr. Donald Sandercock, Fan and Compressor Branch, NASA/Lewis Research Center, for his support and encouragement during this project.

REFERENCES

1. Esgar, G. M., and Sandercock, D. M.: Some Observed Effects of Part-Span Dampers on Rotating Blade Row Performance Near Design Point. NASA TM X-2696, 1973.

2. Roberts, W. B.: Correlation of Part-Span Damper Losses Through Transonic Rotors Operating Near Design Point. NASA TM X-3542, 1977.

3. Roberts, W. B., Crouse, J. E., and Sandercock, D. M.: Off-Design Correlation for Losses due to Part-Span Dampers on Transonic Rotors. NASA TP 1693, 1980.

4. Roberts, W. B.: Aerodynamic Optimization of Part-Span Dampers for Transonic Fans using Area Ruling Concepts. Report to NASA, NEAR TR 216, Nov. 1980.

5. Pope, A. and Goin, K. L.: HIGH SPEED WIND TUNNEL TESTING. John Wiley & Sons, Inc., New York. 1965.

6. Shapiro, A. H.: THE DYNAMICS AND THERMODYNAMICS OF COMPRESSIBLE FLUID FLOW, Vol. 1. The Ronald Press Company, New York. 1953.

7. Schlichting, H.: BOUNDARY-LAYER THEORY, 6th ed. McGraw-Hill Book Company, Inc., New York. 1968.

8. Middagh, R. T.: Optimization and Calibration of the 6 x 6 Inch Supersonic Wind Tunnel. ME-180 Special Projects, San Jose State College Mechanical Engineering Department, San Jose, California. March 1971.

9. Alves, D. F.: An Experimental Investigation of the Shock Wave-Boundary Layer Interaction in a Rectangular Duct. Thesis, San Jose State University, June 1974.

10. Whitcomb, R. T.: A Study of the Zero-Lift Drag-Rise Characteristics of Wing-Body Combination Near the Speed of Sound. NACA Report 1273, Aug. 1952.

11. Sears, W. R.: On Projectiles of Minimum Wave Drag. Quart. Appl. Math, Vol. IV, No. 4, Jan. 1947.

APPENDIXES

A. MODEL AND RAKE DRAWINGS

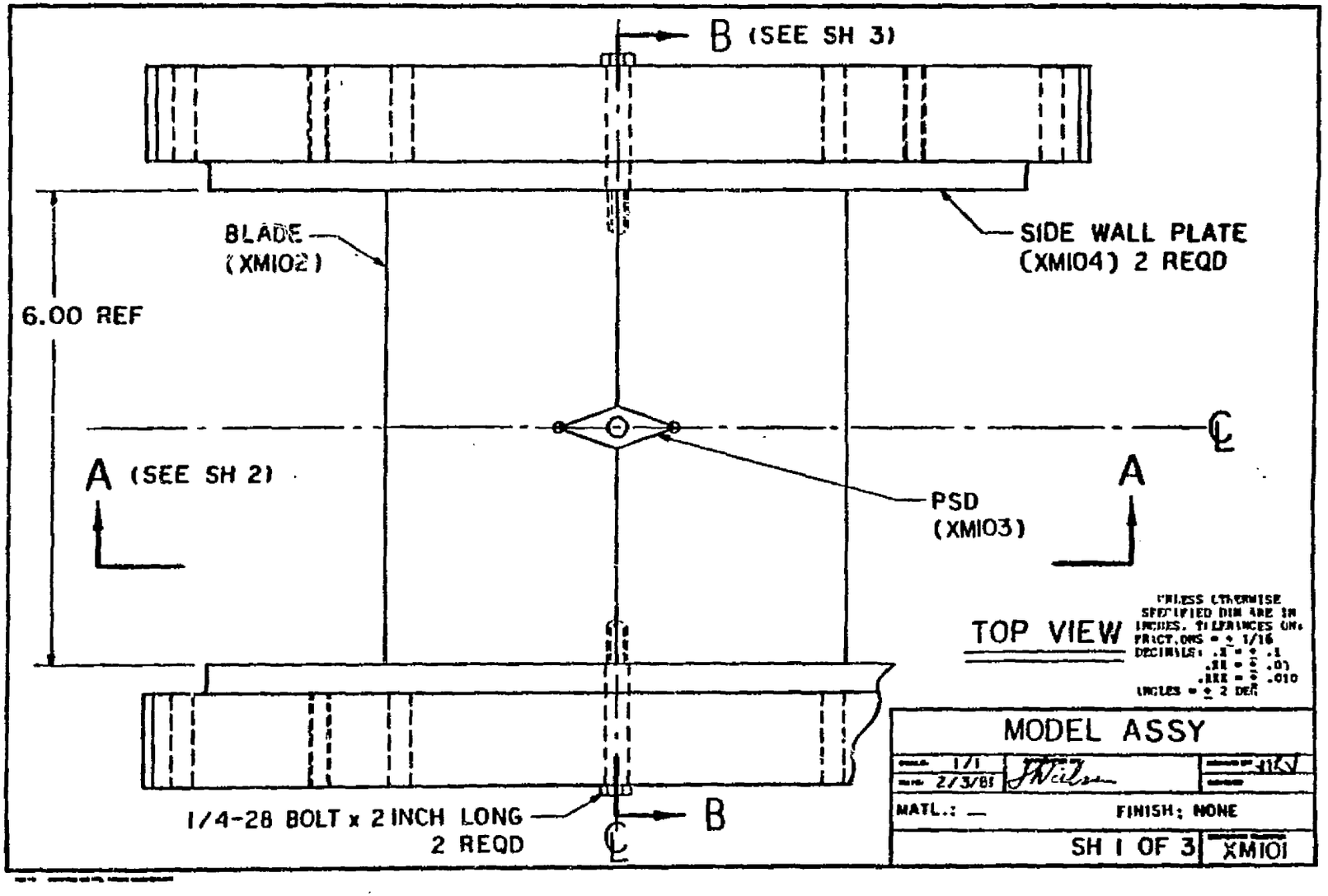

Fig. 32. Model Assembly Drawing, Sheet 1

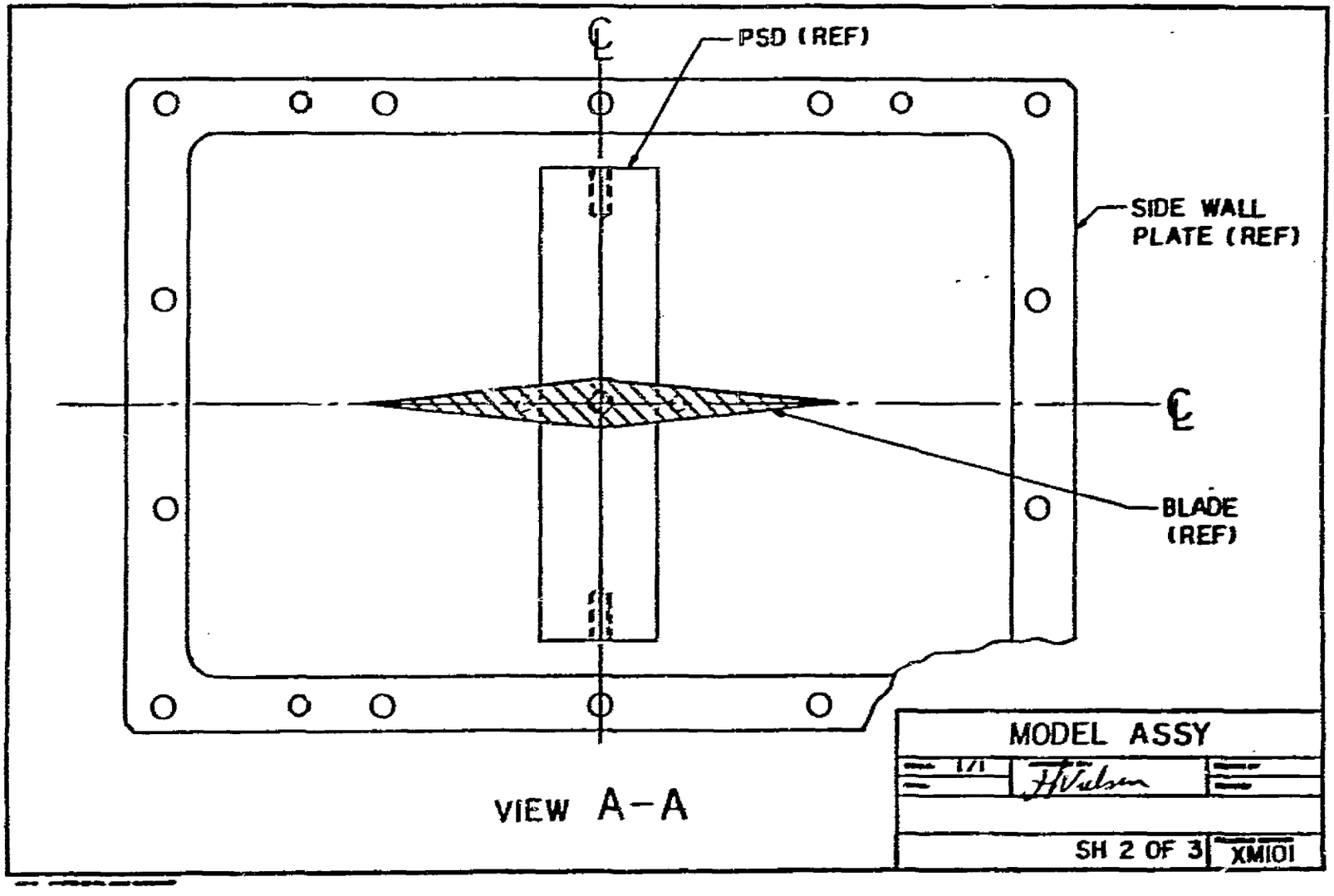

Fig. 32. Continued, Sheet 2

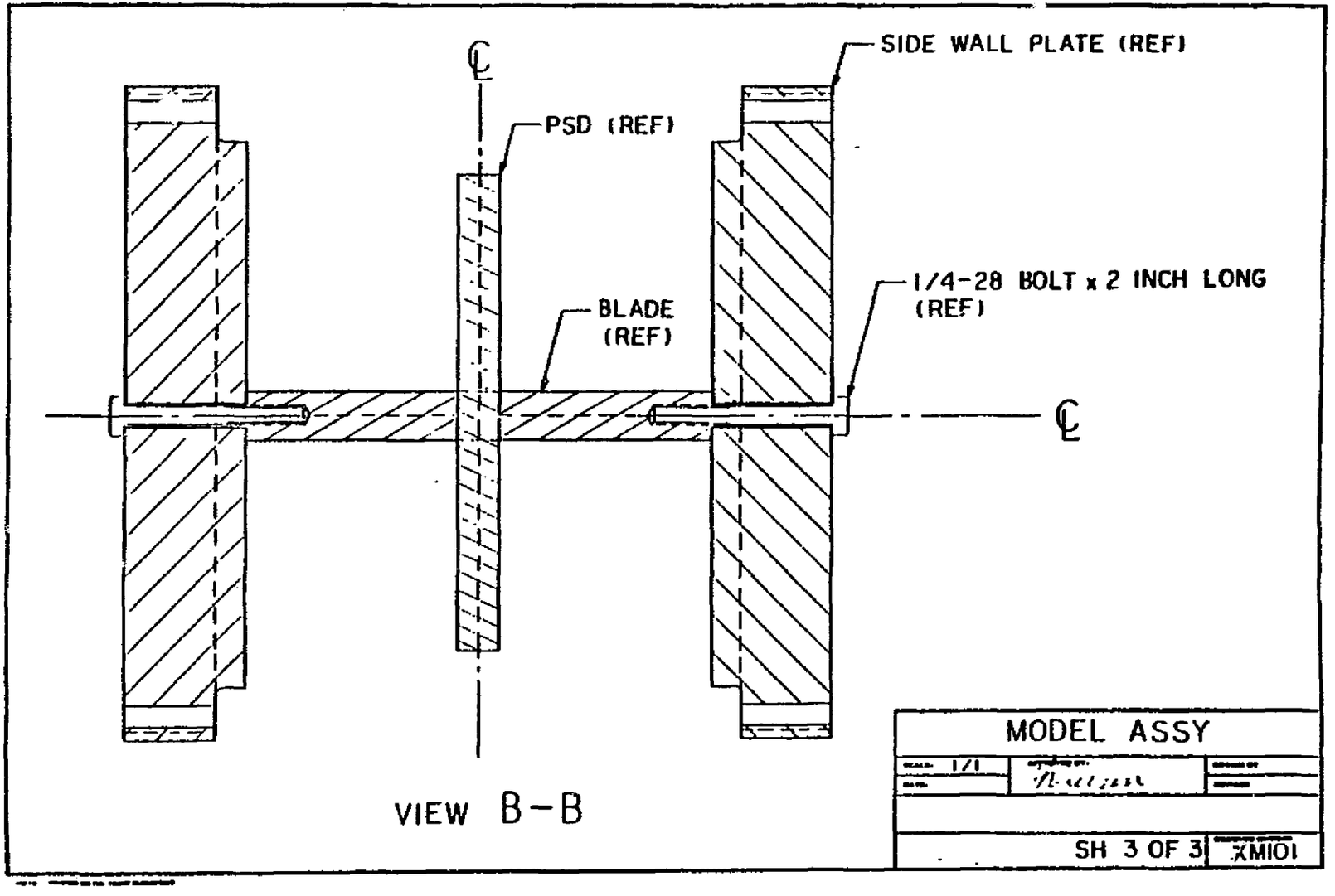

Fig. 32. Continued, Sheet 3

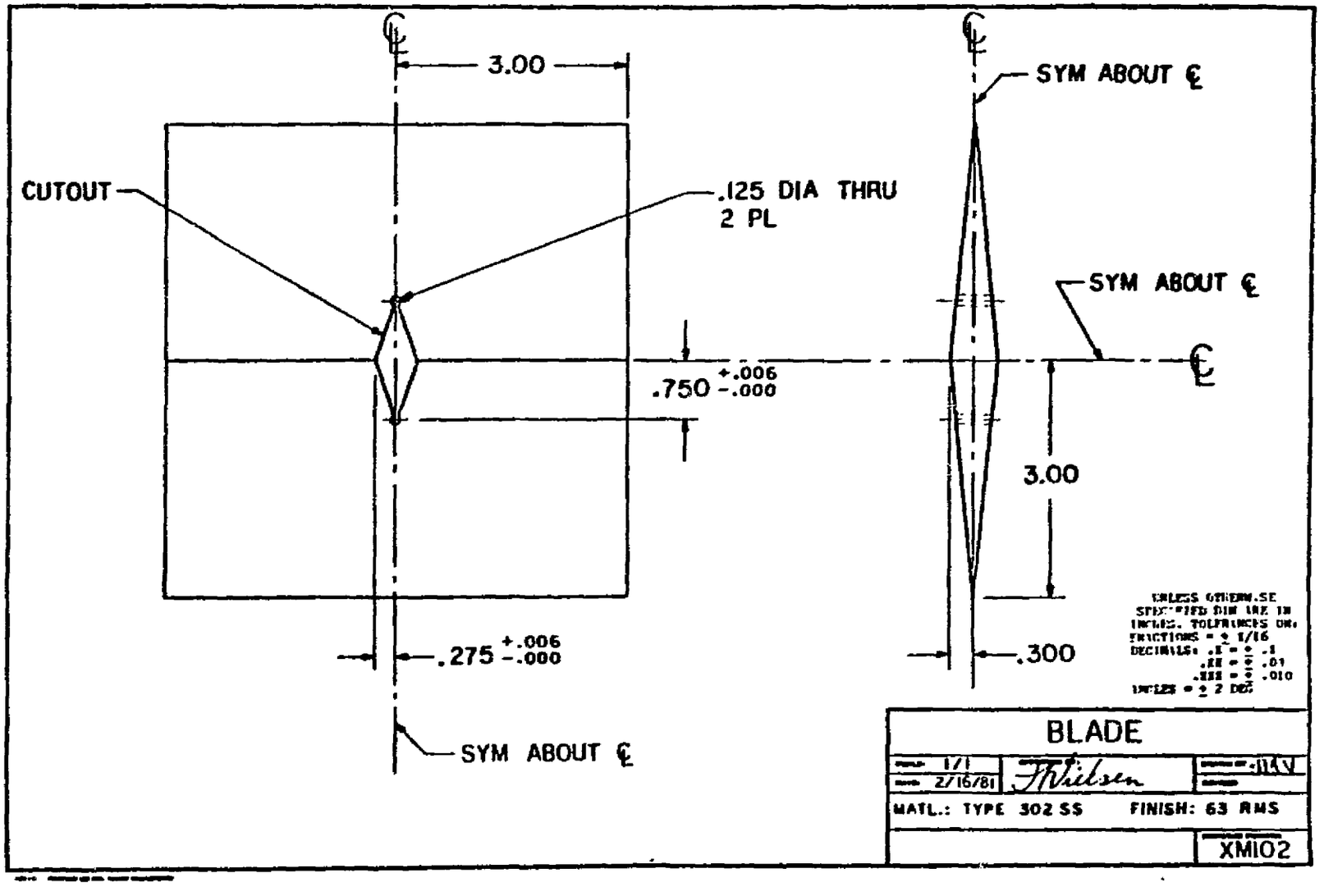

ORIGINAL PAGE IS
OF POOR QUALITY

Fig. 33. Blade Drawing

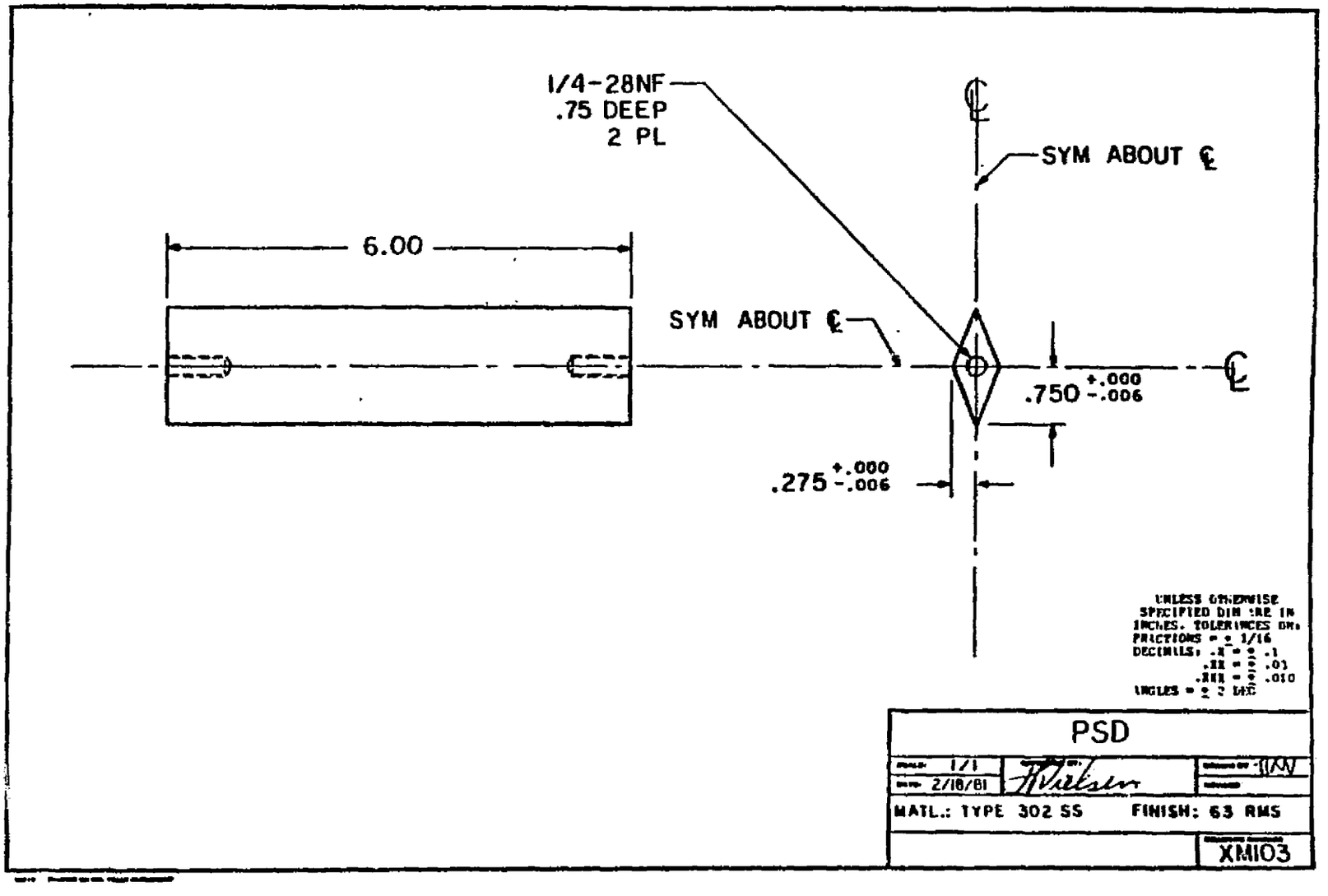

Fig. 34. PSD Drawing

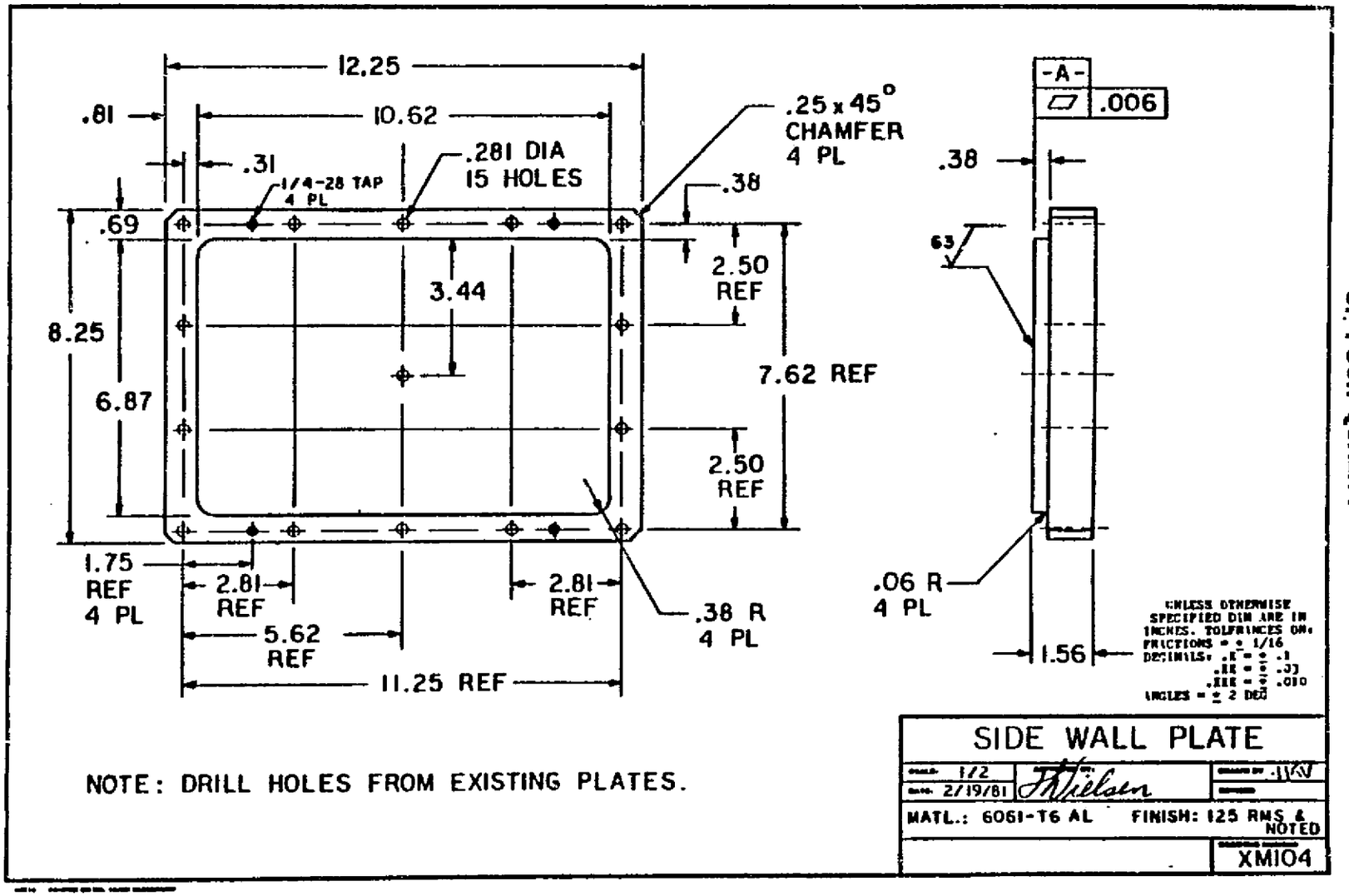

Fig. 35. Side Wall Plate Drawing

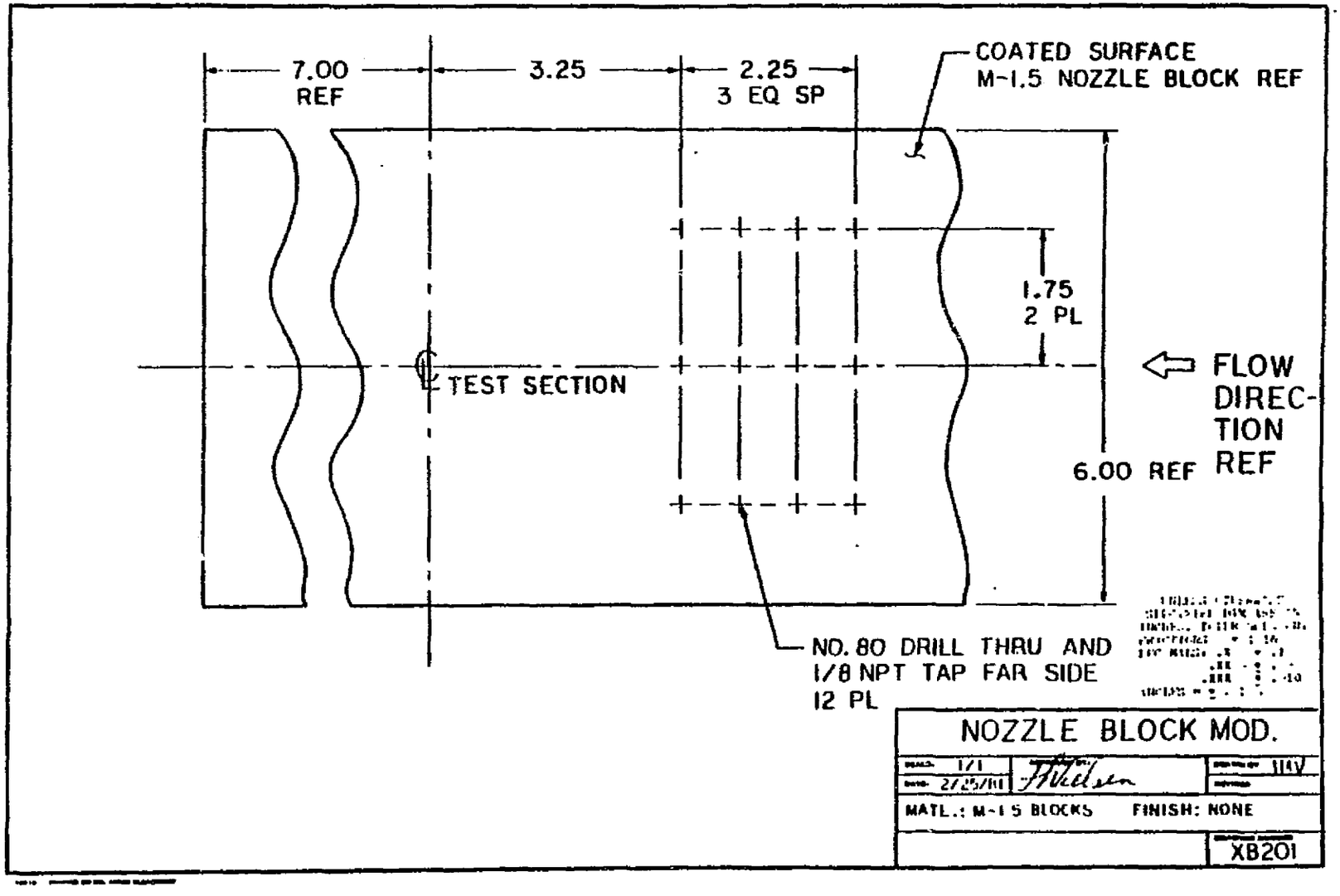

ORIGINAL PAGE IS
OF POOR QUALITY

Fig. 36. Nozzle Block Modification Drawing

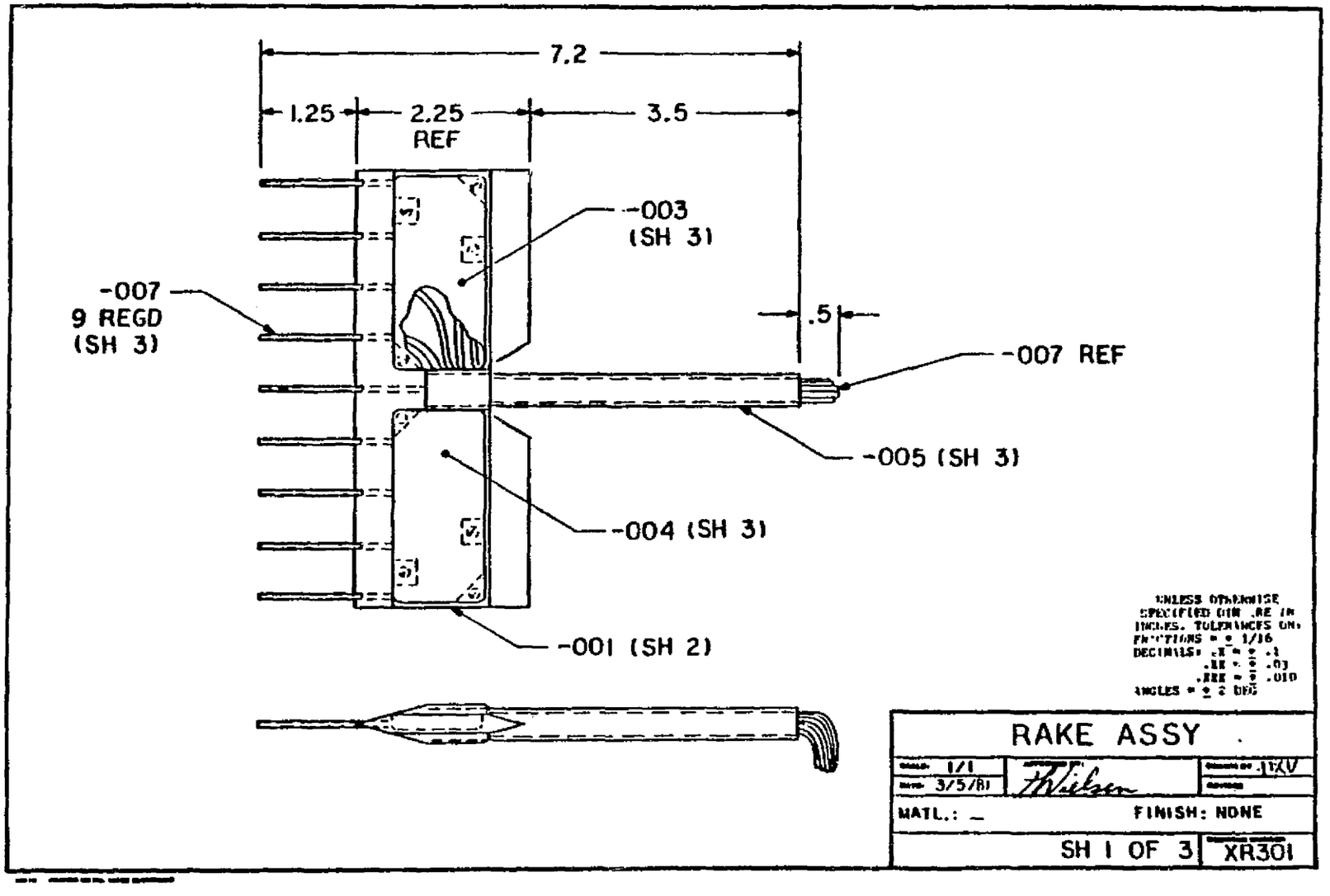

Fig. 37. Rake Assembly Drawing

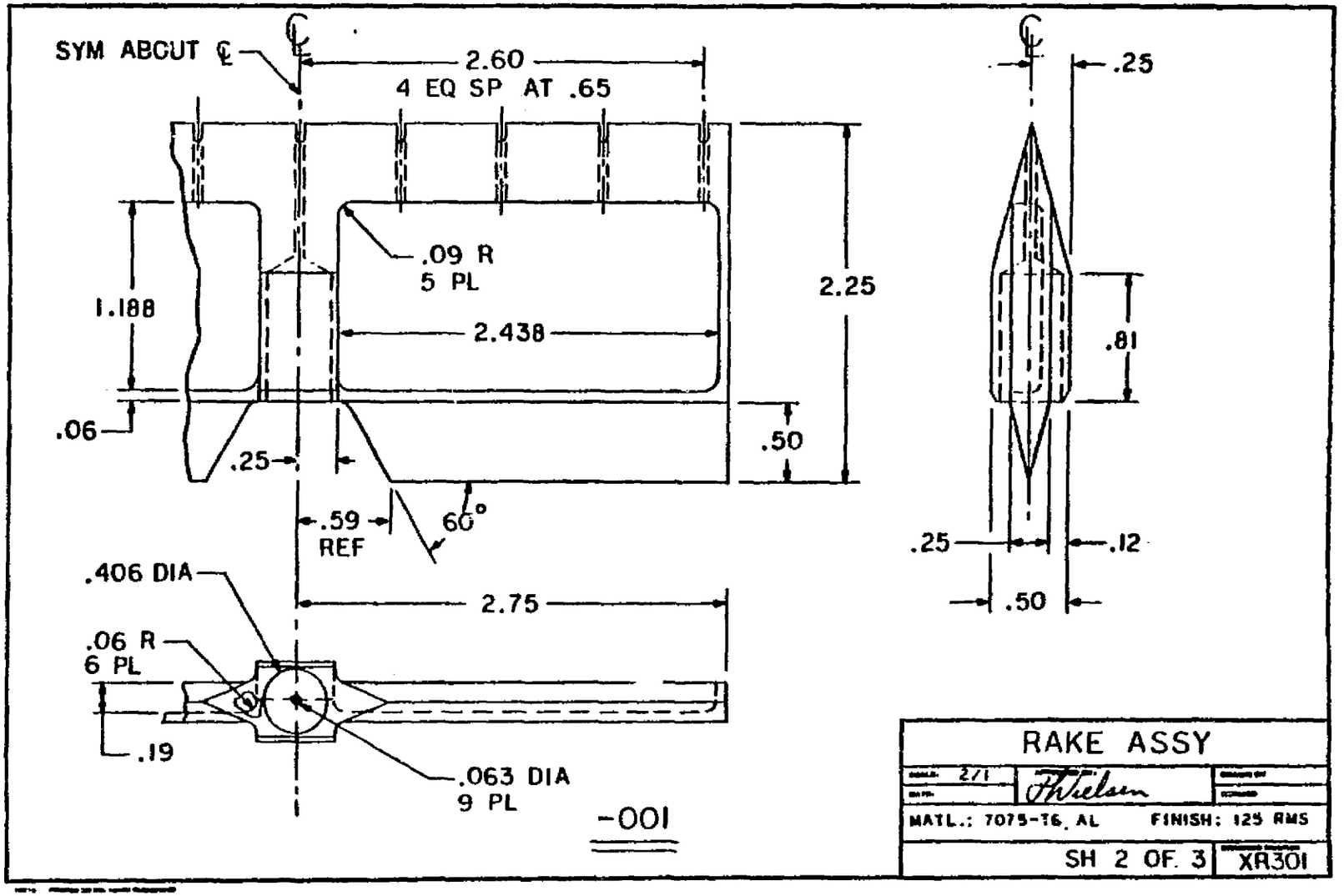

Fig. 37. Continued, Sheet 2

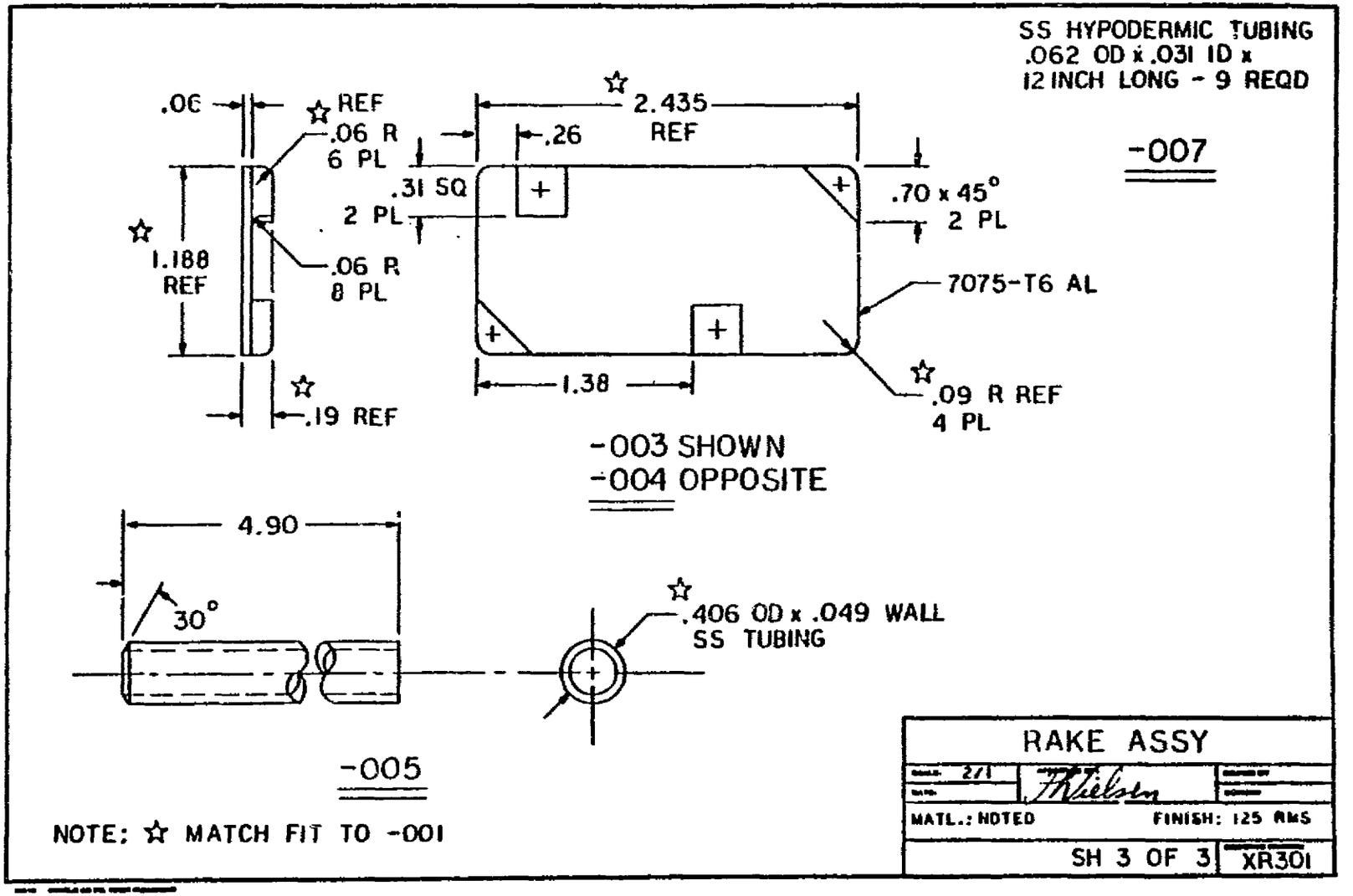

ORIGINAL PAGE IS
OF POOR QUALITY

Fig. 37. Continued, Sheet 3

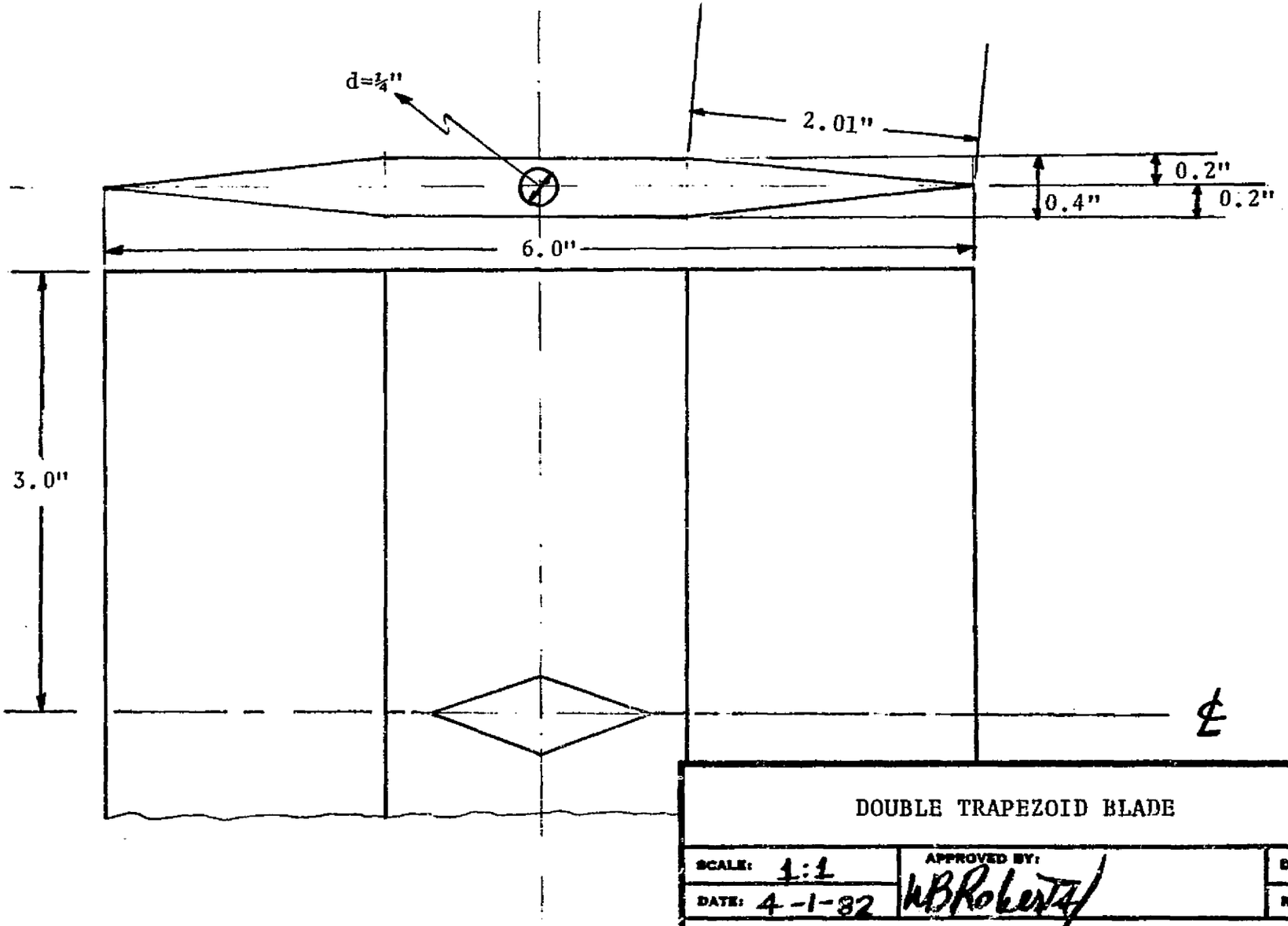

ORIGINAL PAGE IS
OF POOR QUALITY

DOUBLE TRAPEZOID BLADE

SCALE: 1:1	APPROVED BY: HBRoberts	DRAWN BY GR
DATE: 4-1-82		REVISED
		DRAWING NUMBER 1

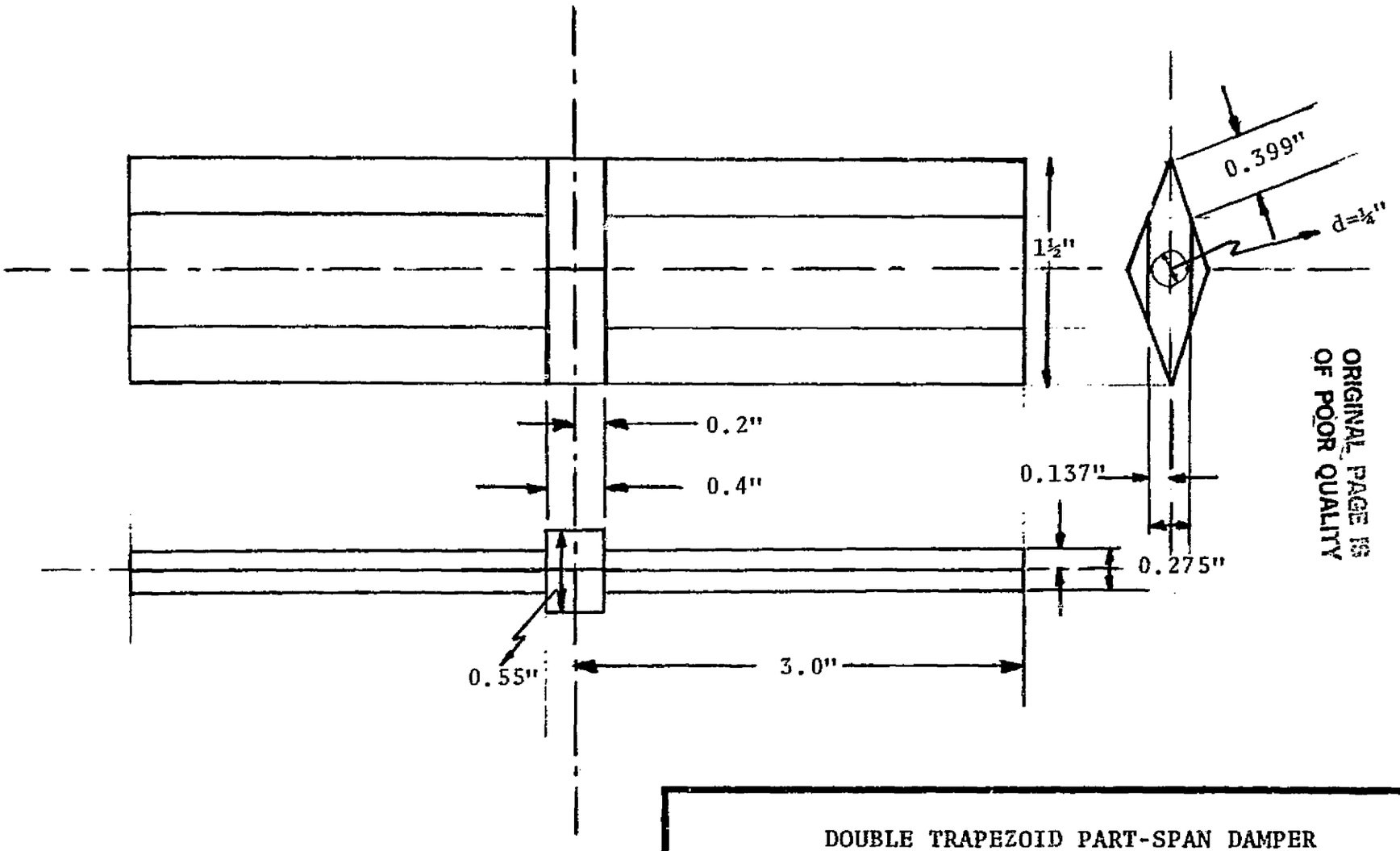

ORIGINAL PAGE IS
OF POOR QUALITY

DOUBLE TRAPEZOID PART-SPAN DAMPER

SCALE: 1:1	APPROVED BY: UBRoberts	DRAWN BY GR
DATE: 4-1-82		REVISED
		DRAWING NUMBER 2.

8½X11 PRINTED ON NO. 1000H CLEARPRINT

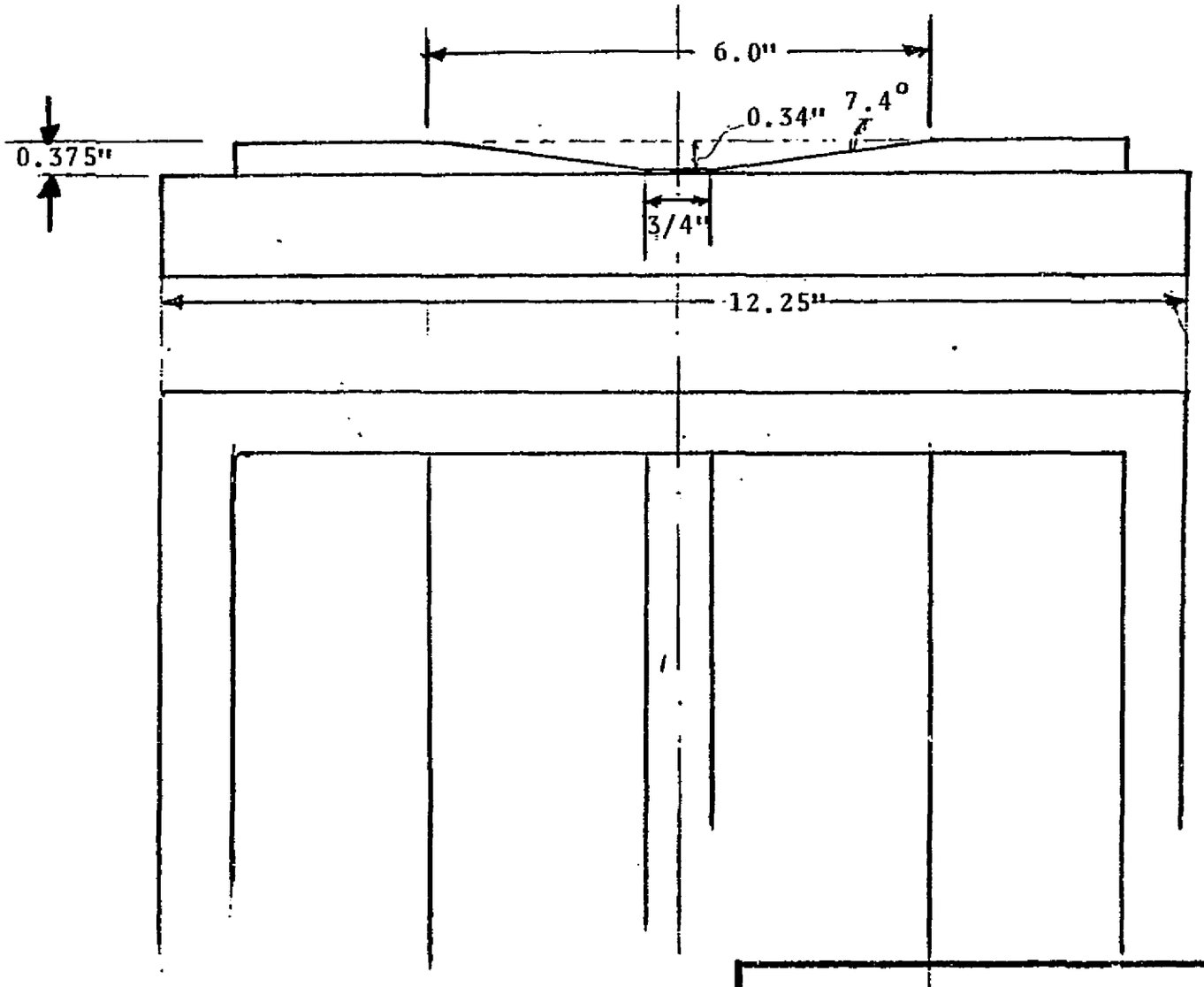

ORIGINAL PAGE IS
OF POOR QUALITY

SIDE PLATES WITH DAMPER AND BLADE AREA RULING

SCALE: 1 : 2	APPROVED BY: W B Roberts	DRAWN BY G-R
DATE: 5/17/82		REVISED
		DRAWING NUMBER

B. CALIBRATION DATA

B. CALIBRATION DATA

The Scanivalve transducer was calibrated in the following manner: First, positive pressure readings were obtained by applying shop air pressure to the transducer. The applied pressure, by means of a pressure regulator, was read on a single tube mercury manometer which was connected to the pressure line. The transducer was further connected to the Sanborn recorder through a charge amplifier. The applied pressures were recorded by a needle deflection, which had to be converted according to the scale setting as shown:

POSITIVE SCANIVALVE TRANSDUCER READINGS

No.	Single tube Manometer (" H_g)	Conversion (psi)	Recorder needle deflection (mm)	Scale 0.05 V/mm	Conversion (V)
1	50.52	24.81	26.3		1.315
2	49.40	24.26	25.9		1.295
3	45.37	22.29	23.6		1.180
4	42.94	21.09	22.5		1.125
5	40.64	19.96	21.1		1.055
6	36.37	17.86	19.0		0.950
7	33.57	16.49	17.5		0.875
8	31.27	15.36	16.3		0.815
9	26.35	12.94	13.8		0.690

No.	Single tube Manometer (" H_g)	Conversion (psi)	Recorder needle deflection (mm)	Scale 0.05 V/mm	Conversion (V)
10	21.35	10.49	11.1		0.555
11	13.22	6.49	6.9		0.345
12	7.22	3.55	4.0		0.200
13	3.57	1.75	2.0		0.100
14	2.99	1.47	1.5		0.075
15	5.35	2.63	2.8		0.140
16	8.97	4.41	4.6		0.230
17	12.15	5.97	6.5		0.325
18	15.42	7.57	8.2		0.410
19	18.87	9.27	10.0		0.500
20	21.59	10.60	11.5		0.575
21	23.59	11.59	12.4		0.620
22	26.57	13.05	13.9		0.695
23	29.58	14.53	15.8		0.790
24	32.85	16.14	16.9		0.845
25	35.97	17.67	18.4		0.920
26	39.10	19.21	20.1		1.005
27	41.65	20.46	21.6		1.080
28	44.17	21.70	22.9		1.145
29	46.54	22.86	24.3		1.215
30	48.07	23.61	24.9		1.245
31	50.17	24.64	26.1		1.305

To continue reading in the negative pressure range, the single tube manometer was replaced by a 18 inch open U-tube manometer. Negative pressures were obtained by using a Ventury tube operated by shop air, and these pressures were read off the U-manometer. The results shown below are:

NEGATIVE SCANIVALVE TRANSDUCER READINGS

No.	U-manometer ($"H_g$)	Conversion (psi)	Recorder needle deflection (mm)	Scale 0.01 V/mm	Conversion (V)
1	-2.24	-1.10	-5.7		-0.057
2	-4.18	-2.05	-10.4		-0.104
3	-5.42	-2.66	-13.7		-0.137
4	-6.34	-3.11	-16.1		-0.161
5	-7.60	-3.73	-19.6		-0.196
6	-8.72	-4.28	-22.4		-0.224
7	-10.00	-4.91	-25.5		-0.255
8	-10.82	-5.31	-28.0		-0.280
9	-11.80	-5.80	-30.6		-0.306
10	-12.80	-6.29	-33.3		-0.333
11	-13.56	-6.66	-35.0		-0.350
12	-14.00	-6.88	-36.2		-0.362
13	-14.34	-7.04	-36.8		-0.368
14	-15.20	-7.47	-39.4		-0.394

For finding the least square fit, the positive and negative pressure summations are:

$$N = 45$$
$$\sum P = 337.42$$
$$\sum P^2 = 8437.561$$
$$\sum V = 20.093$$
$$\sum PV = 447.194$$

Assuming that the errors in the P readings are negligible, the equation is

$V = aP + b$ and the normal equations are:

$$a\sum P^2 + b\sum P = \sum PV \qquad (1)$$
$$a\sum P + b\,N = \sum V \qquad (2)$$

and substituting the above values,

$$a(8437.561) + b(377.42) = 447.194 \qquad (1)$$
$$a(377.42) + b(45) = 20.093 \qquad (2)$$

From (2), $a = (20.093 - 45b)/ 377.42$

and substituting into (1):

$$((20.093 - 45b)/377.42)(8437.561) + b(377.42) = 477.194$$

$$449.195 - 1006.011\ b + b(377.422) = 447.194$$

$$-628.589\ b = 447.194 - 449.195$$

$$b = -2.001/-628.589 = 0.003$$

and substituting b into (2) gives,

$$a = (20.093 - 45(0.003))/377.42 = 0.053$$

and thus $V = 0.053\ P + 0.003$ for the scanner valve pressure transducer, containing a standard deviation of S = 0.127

For calibrating the stagnation chamber transducer a deadweight tester was used. Several readings were taken as shown on the next page.

STAGNATION CHAMBER TRANSDUCER READINGS

Deadweight tester (psi)	Recorder needle deflection (mm)		
	Data 1	Data 2	Average
5	3.6	4.0	3.8
10	7.7	7.6	7.65
15	11.3	11.4	11.35
20	15.1	15.3	15.2
25	19.2	19.2	19.2
30	23.0	23.1	23.05
35	27.1	27.3	27.2
40	30.5	30.5	30.5
45	35.0	35.2	35.1
50	38.6	38.2	38.4
50	38.5	38.6	38.55
45	34.6	34.6	34.6
40	30.4	30.7	30.55
35	26.7	27.1	26.9
30	23.7	23.4	23.55
25	19.5	19.4	19.45
20	15.8	15.7	15.75
15	12.0	11.9	11.95
10	8.2	8.2	8.2
5	4.0	4.2	4.1

No.	Dead weight tester (psi)	Averaged recorder needle deflection (mm)	Scale 0.05 V/mm	Corr. fact. 1.0154	Con-version (v)
1	5	3.95			0.200
2	10	7.92			0.402
3	15	11.65			0.591
4	20	15.47			0.786
5	25	19.32			0.981
6	30	23.30			1.183
7	35	27.05			1.373
8	40	30.52			1.550
9	45	34.85			1.769
10	50	38.47			1.953

The above data was averaged from the readings taken witn the deadweight tester for more accuracy.

To apply a least square fit to the stagnation transducer data, the obtained summations are:

$$N = 10$$
$$\sum P = 275$$
$$\sum P^2 = 9625$$
$$\sum V = 10.790$$
$$\sum PV = 376.992$$

and again assuming that the errors in the P readings are negligible the equation is the same as used before

$V = aP + b$ and the normal equations also:

$$a\sum P^2 + b\sum P = \sum PV \qquad (3)$$
$$a\sum P + b\,N = \sum V \qquad (4)$$

and substituting the above values,

$$a(9625) + b(275) = 376.992 \qquad (3)$$
$$a(275) + b(10) = 10.790 \qquad (4)$$

From (4) $a = (10.709 - 10\,b)/275$

and substituting into (3)

$$((10.790 - 10\ b)/275)(9625) + b(275) = 376.992$$

$$377.664 - 350\ b + 275\ b = 376.992$$

$$b = (376.992 - 377.664)/(-75) = 0.009$$

and substituting this into (4) gives,

$$a = (10.790 - (10)0.009)/275 = 0.039$$

and thus $\underline{V = 0.039\ P + 0.009}$ for the stagnation pressure transducer, with standard deviation of $S = 0.178$

The scanner valve and stagnation calculated voltage equations are plotted on the graph. The actual readings are shown for comparison.

The formula used for reducing the Sanborn recorder strips is derived as follows:

From the stagnation pressure transducer

$$V = 0.039\ P + 0.009$$

$$P = (V - 0.009)/0.039 = 25.707\ V - 0.231$$

V is the voltage output of the transducer recorded on the output strips with a needle deflection of 0.05 V/mm

$$25.707\ V = 25.707 \times 0.05 \times (\text{mm})$$

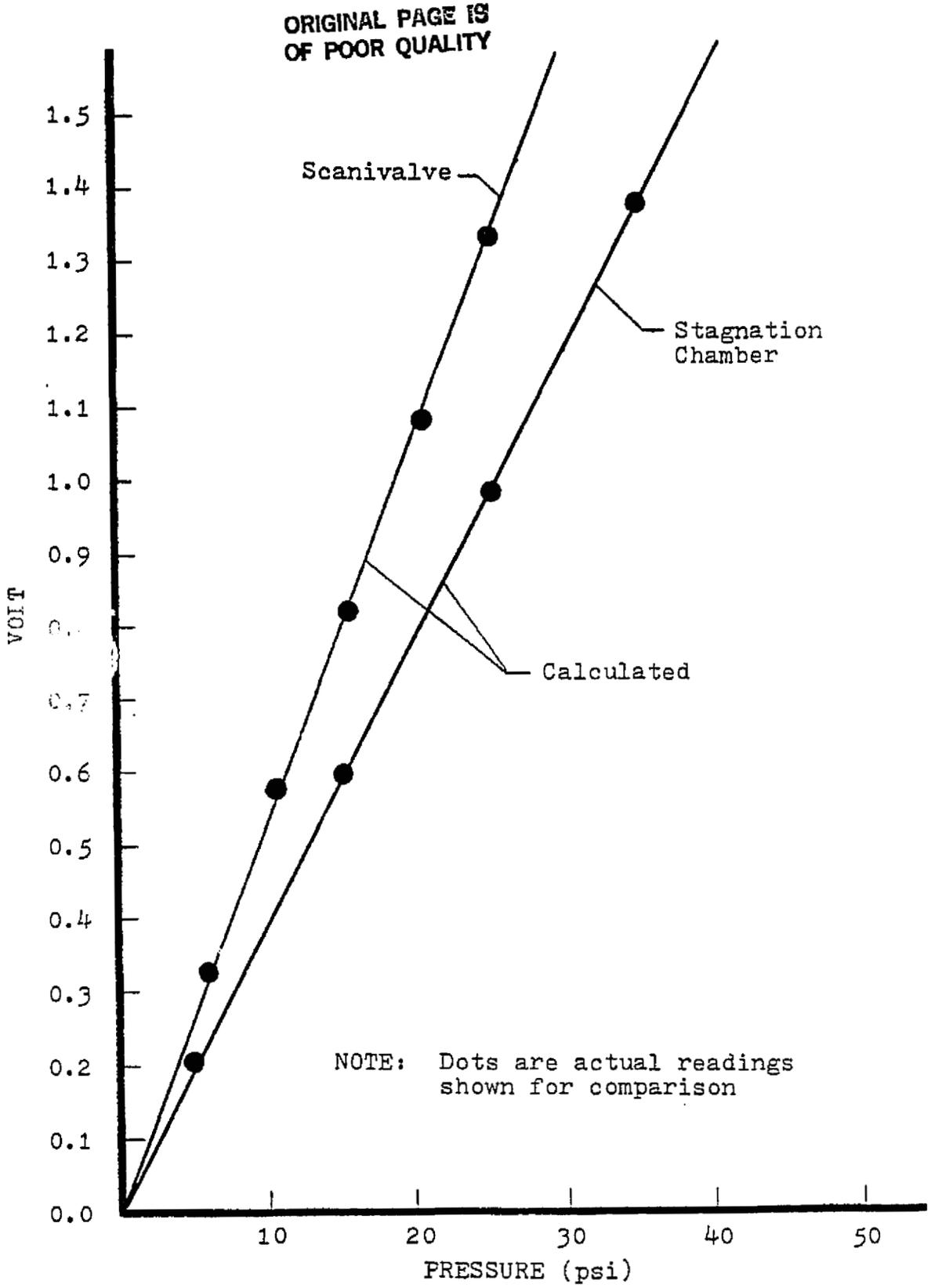

Fig. 38. Transducer Calibration Curves

and $P = 1.285 \times (mm) - 0.231$

adding the barometric pressure of the day (p_b) in which the data was recorded, the absolute pressure reading is,

$$P = 1.285 \times (mm) - 0.231 + P_b$$

For the scanivalve transducer

From $V = 0.053\ P + 0.003$

$$P = (V - 0.003)/0.053 = 18.919\ V - 0.061$$

and similarly

$$18.919\ V = 18.919 \times 0.05 \times (mm)$$

and $P = 0.946 \times (mm) - 0.061 + P_b$

To interpret the dual channel recorder strips for the rake impact pressures the formula used is:

$$P_{rake\ (reduced)} = \frac{P_{scanivalve} + P_b}{P_{stagn.} + P_b} (P_{Ref.Stagn.})$$

$$P_{rake\ (reduced)} \simeq \frac{0.946 \times (mm) - 0.061 + P_b}{1.285 \times (mm) - 0.232 + P_b} (P_{Ref.Stagn.})$$

Since the calculated and the actual graphs of the calibrated transducers are close, the pressure intercepts are ignored. The simplified rake pressure formula thus becomes,

$$P_{rake\ (reduced)} = \frac{0.946 \times (mm) + P_b}{1.285 \times (mm) + P_b} (P_{Ref.Stagn.})$$

The stagnation pressure in the stilling chamber was repeatable in the range of +/- 1 psi due to deviations in the controller. To obtain an area averaged stagnation pressure downstream of the model a fixed upstream stagnation pressure was necessary for the runs in a particular set. Therefore the rake pressures were ratioed to a reference upstream stagnation pressure ($P_{Ref.Stagn.}$). To check the validity of this ratioing, a number of runs were taken with increasing input stagnation pressures. The rake stagnation pressures were found to increase linearly within an error band of 5 percent.

C. TEST DATA

C. TEST DATA

A photographic reduction shows samples (Fig. 39) of the actual recorder strips. All the rake data is tabulated on the following pages.

Pressure data was obtained by first finding the reference line of the recorder needle, subtracting that from the port line deflection in question and storing the number of mm in (B). Similarly, for the stagnation pressure, the difference in mm between the stagnation pressure line (opposite the port) and the reference needle line is (A). The barometric pressure in psi is (C), and the reference stagnation pressure ($P_{Ref.Stagn.}$) is determined by averaging the stagnation pressures of a few strips. All the above information is then substituted into the formula:

$$P_{rake/reduced} = \frac{0.946(B) + (C)}{1.285(A) + (C)} (P_{Ref.Stagn.})$$

For static wall pressures

$$P_s = 0.946(B) + (C) \qquad \text{is used.}$$

For determining Mach numbers

$$\frac{P_s}{P_o} = \frac{0.946(B) + (C)}{1.285(A) + (C)} = X$$

and using this X; the Mach number is found from isentropic flow tables (Ref. 18).

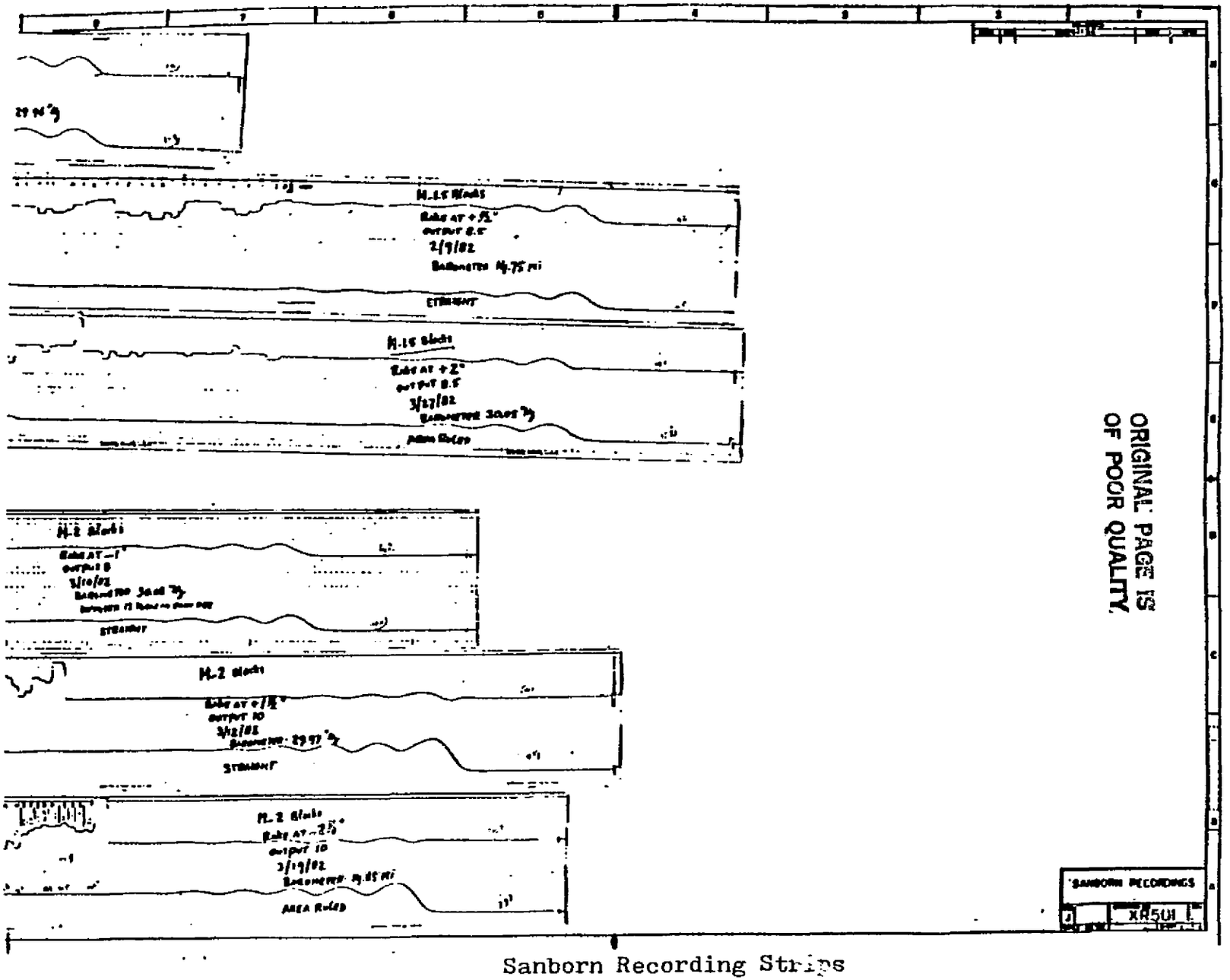

Sanborn Recording Strips

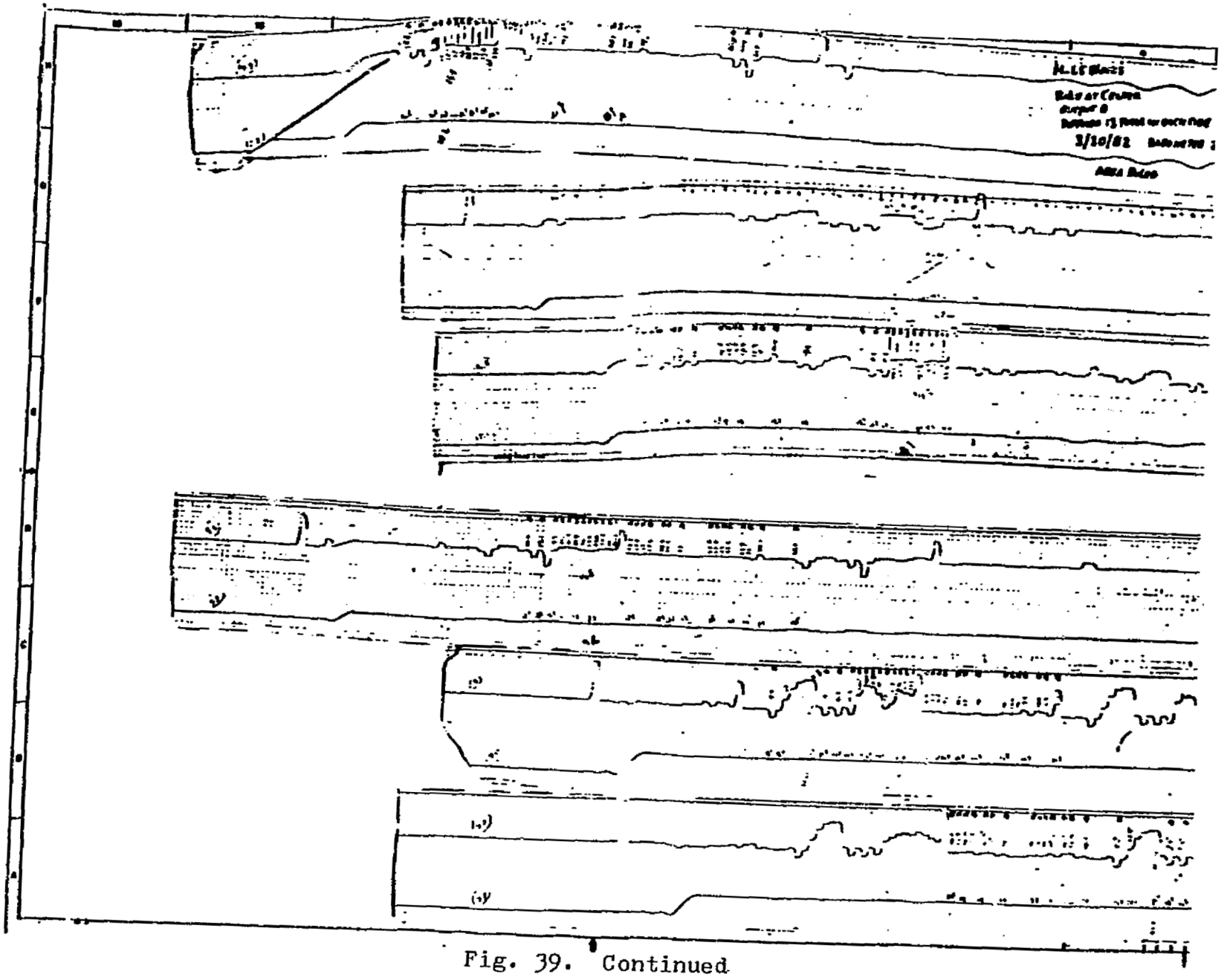

Fig. 39. Continued

ORIGINAL MODEL

M-1.5 nbs / Output gauge: 8 / Subsonic / AR / Diffuser: 13 turns in each side

Date	3/30	-	-	-	-	-	-	-	-	-	-
P_b (psi)	14.72	-	-	-	-	-	-	-	-	-	-
Rake pos. (y")		+2½	+2	+1½	+1	+½	0	-½	-1	-1½	-2	-2½
Rake port No.												
1		27.03	27.17	26.87	26.55	26.89	26.22	27.52	26.90	2 2	26.87	26.56
2		27.03	27.17	26.87	26.55	26.89	26.31	27.39	26.71	26.55	26.87	26.72
3		27.03	27.07	26.96	26.28	26.37	25.82	26.52	25.76	26.43	26.87	26.72
4		26.65	26.69	26.40	25.73	25.77	25.27	25.53	25.67	25.55	26.40	26.59
5		26.46	26.39	26.21	25.67	25.20	24.70	25.44	25.57	25.66	26.21	26.08
6		26.84	26.84	26.59	25.94	25.48	25.13	25.72	26.05	25.66	26.59	26.36
7		27.03	27.13	26.93	26.77	26.61	25.95	26.91	26.81	26.13	26.68	26.68
8		27.03	27.23	26.93	26.95	26.93	26.22	27.29	26.90	26.40	26.68	26.59
9		26.46	26.75	26.84	26.77	26.67	25.95	26.94	26.52	26.13	26.49	25.85

ORIGINAL MODEL

M-1.5 nbs / Output gauge: 8.5 / Transonic / Choked condition

Date	2/16	2/9	-	-	-	2/11	2/10	2/11	-	-	2/16
P_b (psi)	14.85	14.75	-	-	-	14.82	14.75	14.82	-	-	14.85
Rake pos. (y")	+2½	+2	+1½	+1	+½	0	-½	-1	-1½	-2	-2½
Rake port No.											
1	24.60	24.70	25.39	25.49	24.91	23.02	25.65	24.94	25.74	25.66	25.17
2	25.20	24.52	24.79	25.30	25.58	21.56	26.04	25.23	25.95	25.76	25.96
3	25.40	25.72	25.98	25.40	23.68	20.20	23.89	25.02	26.25	26.89	25.96
4	25.70	25.05	24.43	20.95	16.81	15.88	15.89	18.65	23.39	24.82	25.57
5	22.41	18.32	18.53	16.61	14.89	14.97	13.94	15.16	17.55	19.02	20.02
6	26.09	25.67	25.40	22.89	18.56	17.42	17.94	20.59	24.64	26.36	26.03
7	25.40	24.86	25.78	25.30	25.48	21.11	24.67	26.00	26.45	26.30	26.23
8	25.40	23.56	24.79	25.01	25.58	22.72	25.94	25.51	25.83	25.76	25.83
9	24.60	24.35	24.99	25.20	25.10	23.66	25.26	25.70	25.52	25.22	24.42

ORIGINAL MODEL

M-1.5 nbs / Output gauge: 8.5 / Transonic / AR / Choked condition

Date	3/27	-	-	-	-	-	-	-	-	-	-
P_b (psi)	14.76	-	-	-	-	-	-	-	-	-	-
Rake pos. (y")	+2½	+2	+1½	+1	+½	0	-½	-1	-1½	-2	-2½
Rake port No.											
1	24.91	25.73	24.42	24.31	26.34	23.89	25.87	25.29	25.80	25.66	24.99
2	25.59	25.63	24.80	24.60	26.16	23.07	25.87	25.51	25.62	25.84	25.66
3	25.98	26.14	25.55	25.18	25.25	21.30	24.56	25.25	26.18	26.20	26.14
4	26.07	24.51	24.80	21.53	19.80	18.11	18.49	21.33	23.65	25.33	26.01
5	22.58	19.89	19.61	18.15	17.08	16.42	16.62	17.09	19.42	20.87	22.19
6	26.40	26.17	25.62	23.58	21.07	18.96	24.10	22.22	25.24	26.05	25.82
7	26.11	26.17	26.11	25.13	25.55	22.13	24.84	25.42	25.99	26.25	26.01
8	25.76	25.69	25.74	25.65	26.55	22.71	26.09	25.84	25.71	25.54	25.82
9	23.83	25.01	24.98	25.26	25.37	24.72	24.96	25.48	25.24	24.03	23.81

ORIGINAL MODEL

M-2 nbs / Output gauge: 8 / Subsonic / Diffuser: 13 turns in each side

Date	3/9	-	-	-	3/10	-	-	-	-	-
P_b (psi)	14.81	-	-	-	14.78	-	-	-	-	-
Rake pos. (y")	+2½	+2	+1½	+1	+½	0	-½	-1	-1½	-2	-2½
Rake port No.											
1	25.39	25.70	25.36	26.49	26.84	25.50	25.76	25.62	26.05	25.34	24.54
2	25.49	25.99	26.53	26.79	26.93	25.40	26.31	26.30	26.87	26.03	24.73
3	25.49	26.40	26.75	26.86	26.30	25.59	25.66	26.17	26.89	26.06	24.82
4	25.59	26.40	26.17	24.97	24.47	24.54	24.35	24.74	26.12	26.06	24.82
5	25.49	25.48	25.88	24.90	23.84	23.87	23.16	24.17	25.66	25.49	24.47
6	25.49	26.24	26.75	25.81	24.89	24.66	23.98	24.97	26.31	25.89	24.47
7	25.49	26.34	26.85	26.91	26.68	25.58	25.91	26.59	26.93	25.89	24.47
8	25.32	25.96	26.85	26.91	26.81	25.60	26.43	26.24	26.59	26.09	24.56
9	25.02	25.30	25.23	25.72	22.54	25.24	25.60	25.15	25.20	25.30	24.10

ORIGINAL MODEL

M-2 nbs / Output gauge: 10 / Supersonic / Choked condition

Date	3/12	-	-	-	-	-	-	-	-	-	-
P_b (psi)	14.72	-	-	-	-	-	-	-	-	-	-
Rake pos. (y")		$+2\frac{1}{2}$	+2	$+1\frac{1}{2}$	+1	$+\frac{1}{2}$	0	$-\frac{1}{2}$	-1	$-1\frac{1}{2}$	-2	$-2\frac{1}{2}$
Rake port No.												
1	26.40	27.55	29.82	28.82	32.08	22.07	32.63	31.96	30.19	28.20	25.54
2	26.88	30.77	31.55	32.47	31.23	18.29	30.57	34.75	36.76	36.23	28.46
3	28.40	32.48	34.03	28.73	23.70	16.40	27.04	29.17	33.62	35.75	30.89
4	28.31	32.95	22.07	17.35	13.34	13.57	13.69	17.08	21.57	31.25	32.35
5	29.25	28.30	17.65	14.53	12.77	12.15	12.71	15.22	17.64	24.83	30.82
6	30.30	34.58	29.82	21.77	16.63	12.62	14.10	19.22	24.81	34.46	32.03
7	28.40	35.91	35.85	29.91	27.47	17.88	26.28	30.29	33.98	36.06	30.42
8	25.56	32.78	36.79	35.34	33.17	18.35	31.04	34.29	36.94	35.00	28.32
9	24.80	24.38	28.69	29.91	31.71	23.64	30.29	30.57	28.26	26.60	25.31

ORIGINAL MODEL

M-2 nbs / Output gauge: 10 / Supersonic / AR / Choked condition

Date	3/20	3/19	-	-	-	3/20	3/19	-	-	-	-
P_b (psi)	14.82	14.85	-	-	-	14.82	14.85	-	-	-	-
Rake pos. (y")	+2½	+2	+1½	+1	+½	0	-½	-1	-1½	-2	-2½
Rake port No.											
1	22.89	27.91	30.25	30.93	31.79	24.31	31.71	31.98	32.24	28.09	26.14
2	26.40	30.83	34.18	34.07	31.79	19.89	30.74	33.88	36.06	33.96	25.66
3	26.95	33.96	34.67	29.66	27.45	16.69	25.08	27.75	35.49	35.98	29.95
4	29.01	33.76	26.12	17.27	15.90	13.41	13.17	15.73	32.72	33.73	32.34
5	29.94	29.86	19.55	15.22	13.59	12.50	12.49	13.77	19.84	29.20	30.43
6	29.24	35.13	28.40	20.29	15.43	13.35	13.66	15.78	26.52	35.75	31.48
7	27.99	34.54	35.19	30.35	27.45	17.15	23.90	28.04	35.94	35.64	29.09
8	26.87	32.78	35.29	32.78	31.80	20.80	31.61	33.29	36.51	32.84	27.18
9	22.21	26.93	29.86	29.66	29.39	25.46	30.64	30.67	31.29	26.48	23.35

MODIFIED MODEL

M-1.5 nbs/output gauge 10/Transonic/Straight Wall

Date	4/28	-	-	-	-	-	-	-	-	-	-
P_b (psi)	14.76	-	-	-	-	-	-	-	-	-	-
Rake pos. (y")	+2½	+2	+1½	+1	+½	0	-½	-1	-1½	-2	-2½
Rake port No.											
1	32.96	35.06	34.07	33.73	33.77	27.33	33.40	33.81	34.24	34.87	33.15
2	31.19	33.11	31.04	31.01	33.92	29.13	33.78	34.20	33.93	32.80	30.97
3	33.74	34.98	34.54	34.11	34.38	29.28	34.63		34.39	35.02	33.90
4	33.58	34.75	34.07	32.67	31.77	29.99	32.31	32.96	34.01	34.64	33.67
5	31.42	31.16	30.89	28.73	26.46	26.24	26.97	28.49	30.59	30.89	31.20
6	33.74	34.98	34.69	34.04	33.69	30.30	33.78	33.66	34.39	35.10	34.05
7	32.19	34.20	34.46	34.11	34.30	28.42	34.09	33.97	34.31	35.02	33.67
8	29.11	32.25	34.07	34.79	34.84	28.97	34.63	33.89	34.46	34.26	30.82
9	27.95	29.83	30.65	31.16	31.61	31.00	32.39	30.65	29.75	29.51	28.50

MODIFIED MODEL

M-1.5 nbs/output gauge 10/Transonic/AR, Damper

Date	4/30	-	-	-	-	-	-	-	-	-	-
P_b (psi)	14.71	-	-	-	-	-	-	-	-	-	-
Rake pos. (y")	$+2\frac{1}{2}$	+2	$+1\frac{1}{2}$	+1	$+\frac{1}{2}$	0	$-\frac{1}{2}$	-1	$-1\frac{1}{2}$	-2	$-2\frac{1}{2}$
Rake port No.											
1	32.07	34.94	34.04	34.25	33.29	28.17	33.18	34.17	34.29	34.70	31.36
2	31.00	32.81	30.36	30.75	33.20	27.70	32.62	32.91	33.63	32.80	28.14
3	32.58	34.64	34.06	34.02	33.35	27.95	33.30	33.55	33.91	34.70	31.89
4	32.78	34.36	33.60	33.31	31.80	28.61	32.64	33.29	33.54	34.51	31.80
5	30.85	31.69	30.85	30.19	27.76	26.02	26.58	29.66	31.19	31.65	30.33
6	32.34	34.61	33.16	33.31	32.64	29.47	32.69	32.76	33.35	34.18	31.43
7	32.45	34.79	34.01	34.16	33.29	28.91	33.44	33.64	34.66	34.88	31.56
8	32.64	34.73	34.10	34.93	32.76	27.23	32.60	33.84	34.95	35.06	30.17
9	28.85	30.27	31.25	31.93	31.47	27.79	30.87	32.11	30.91	30.13	27.86

MODIFIED MODEL

M-1.5 nbs/output gauge 10/Transonic/AR, Damper & Blade

Date	5/28	-	-	-	-	-	-	-	-	-	-
P_b (psi)	14.70	-	-	-	-	-	-	-	-	-	-
Rake pos. (y")	+2½	+2	+1½	+1	+½	0	-½	-1	-1½	-2	-2½
Rake port No.											
1	26.36	30.04	28.82	27.98	28.32	25.77	29.08	29.74	29.23	28.97	25.92
2	24.83	27.72	25.56	25.46	28.72	27.41	29.55	29.59	28.29	26.44	24.00
3	27.82	30.26	29.09	28.75	28.23	24.75	28.91	29.82	29.17	29.99	26.51
4	27.75	29.89	28.64	28.37	25.95	23.72	26.16	29.07	28.40	29.43	27.63
5	26.44	28.02	26.63	25.95	26.07	25.05	26.40	27.05	28.02	27.79	27.83
6	27.29	30.34	29.31	28.76	28.68	26.61	29.00	29.74	28.98	29.50	27.97
7	25.14	29.97	30.48	30.14	29.96	28.65	30.83	31.24	30.38	29.55	24.99
8	23.60	27.87	28.84	29.55	29.25	27.04	29.27	29.74	28.64	25.79	23.61
9	22.30	24.80	24.95	24.71	24.13	23.15	24.69	25.03	23.98	23.09	22.07

MODIFIED MODEL

M-2.0 nbs/output gauge 10/Supersonic/Straight Wall

Date	7/15	-	-	-	-	-	-	-	-	-	-
P_b (psi)	14.70	-	-	-	-	-	-	-	-	-	-
Rake pos. (y")	+2½	+2	+1½	+1	+½	0	-½	-1	-1½	-2	-2½
Rake port No.											
1	24.41	25.32	21.27	18.83	20.62	19.26	24.24	24.33	26.48		25.76
2	20.01	28.72	20.58	17.11	24.24	12.73	23.78	23.09	28.35		25.09
3	24.00	28.78	25.99	25.52	25.84	17.67	25.80	28.23	28.20		25.35
4	22.62	25.70	24.97	24.21	28.02	19.77	29.61	24.96	26.19		24.08
5	21.36	21.58	22.49	22.50	23.94	23.50	24.72	22.04	22.00		23.76
6	28.26	26.81	25.59	25.74	26.21	17.59	27.35	25.44	25.57		28.02
7	24.65	30.32	27.38	29.51	28.08	16.17	25.56	27.14	27.03		25.51
8	23.60	24.60	24.06	23.74	24.52	16.83	24.76	25.91	27.78		24.87
9	21.82	23.33	19.23	16.60	23.78	14.38	25.57	18.27	17.94		24.63

MODIFIED MODEL

M-2.0 nbs/output gauge 10/Supersonic/AR, Damper & Blade

Date	6/20	-	-	-	-	-	-	-	-	-	-
P_b (psi)	14.72	-	-	-	-	-	-	-	-	-	-
Rake pos. (y")		+2½	+2	+1½	+1	+½	0	-½	-1	-1½	-2	-2½
Rake port No.												
1		29.52	30.25	28.02	24.57	29.16	24.81	28.79	33.43	33.88		29.57
2		25.02	19.43	21.96	22.63	25.35	18.21	28.60	30.90	31.67		27.74
3		32.04	33.49	28.52	30.62	38.68	18.66	31.38	32.93	32.37		32.33
4		29.96	28.58	27.09	28.84	33.31	15.61	13.58	27.21	31.02		33.06
5		27.42	27.61	29.29	26.95	28.59	27.25	16.25	18.14	24.27		24.31
6		32.43	29.45	29.03	28.24	30.14	28.16	26.28	29.10	31.11		22.64
7		34.11	25.45	31.83	26.68	30.68	17.60	30.07	32.84	33.45		31.68
8		28.44	33.63	26.60	26.79	26.74	19.66	27.31	30.01	30.62		30.46
9		23.27	23.07	21.28	19.98	18.07	18.80	24.07	20.36	18.23		26.16

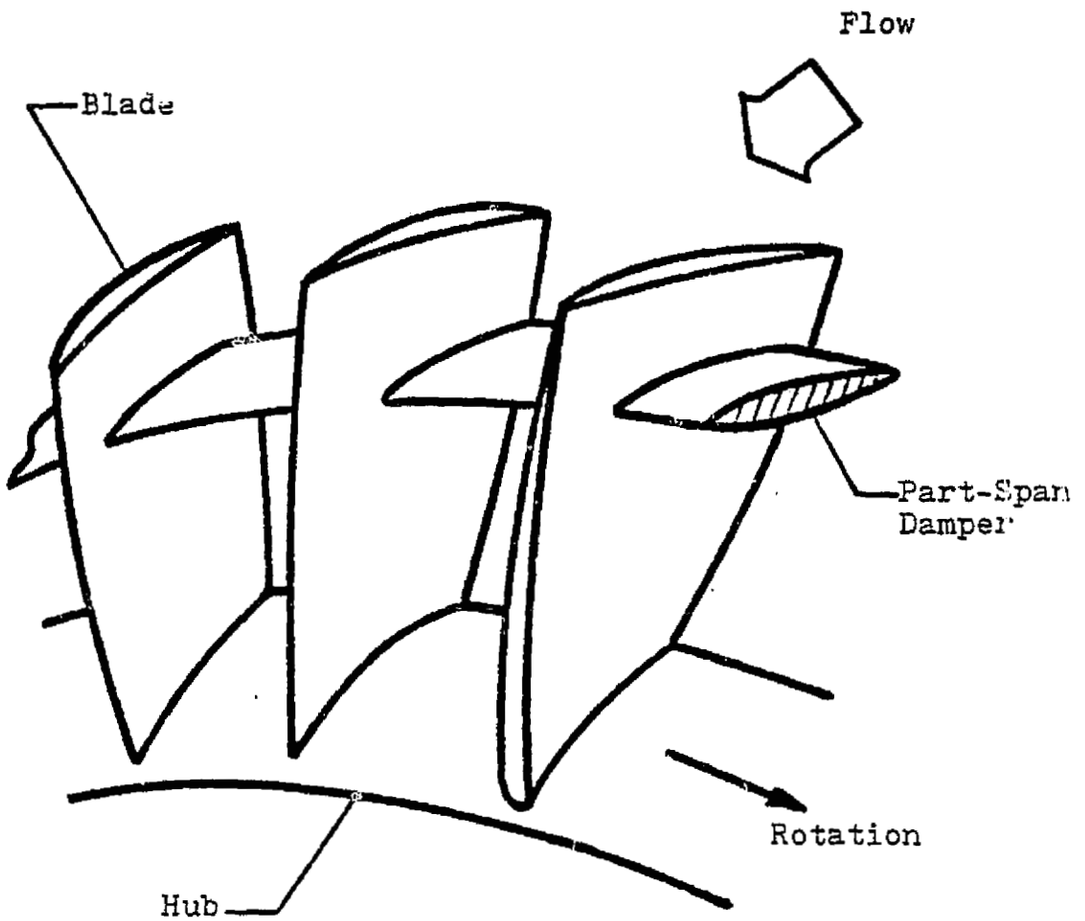

Fig. 1. Rotor-Blade Row with Part-Span Dampers

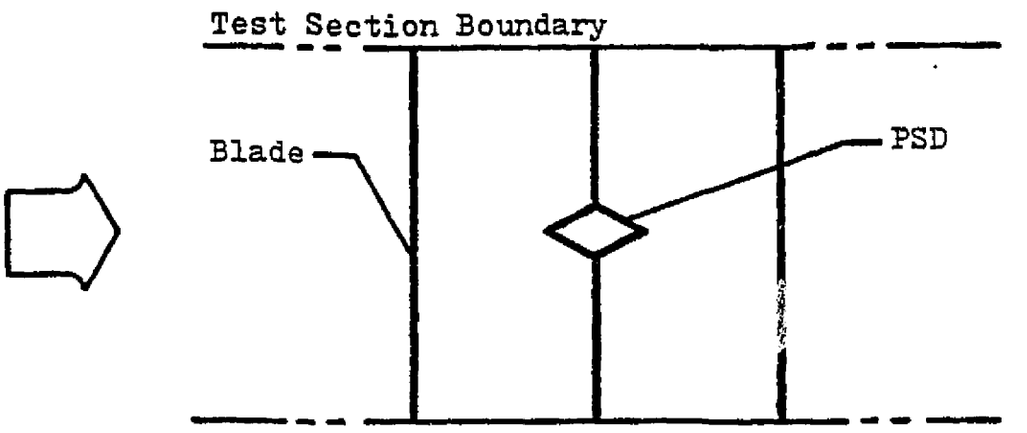

TOP VIEW

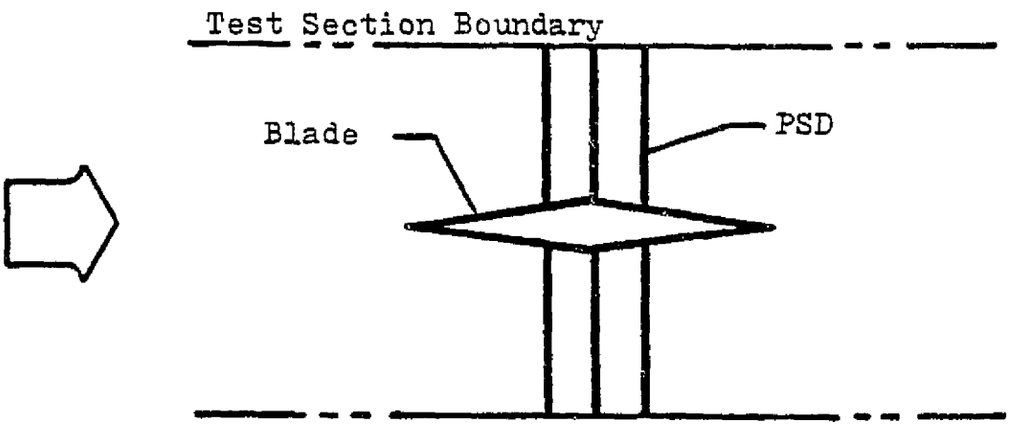

SIDE VIEW

Fig. 2. Model Configuration

ORIGINAL PAGE
COLOR PHOTOGRAPH

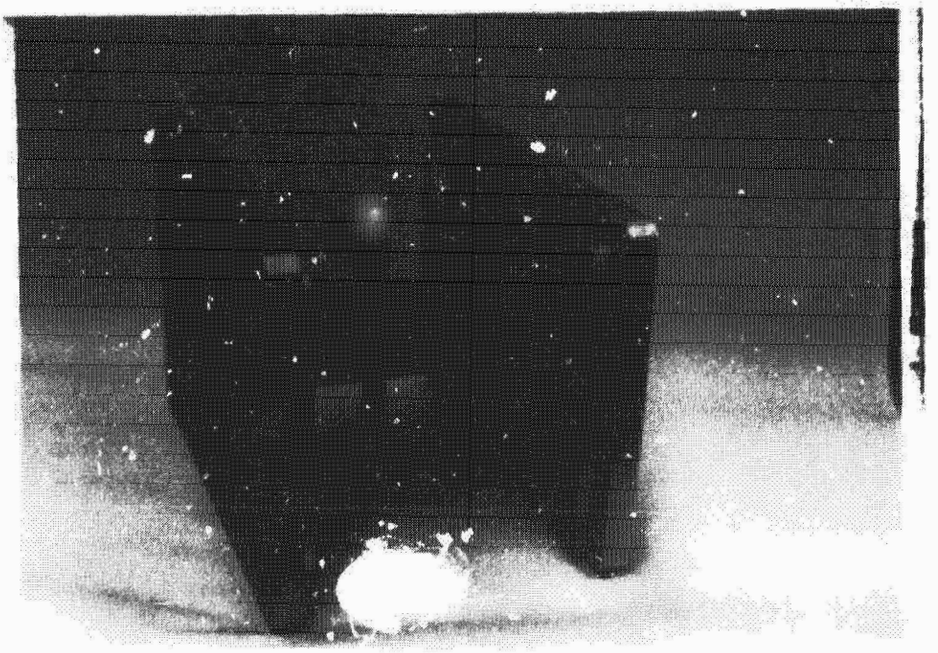

FIGURE 3. Test Model -
Straight Configuration

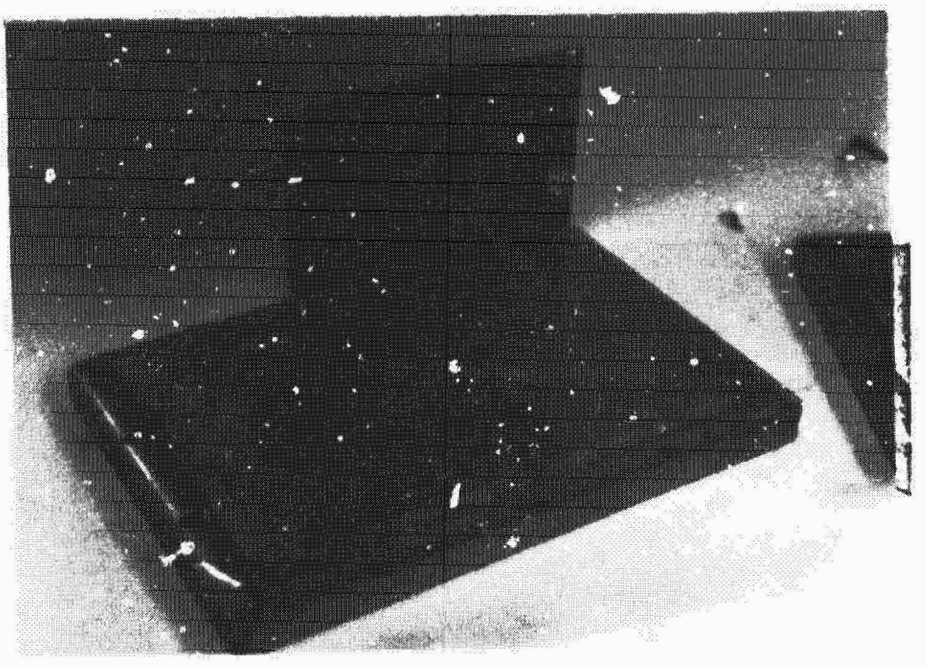

FIGURE 4. Test Model -
Area Ruled for Damper

ORIGINAL PAGE
COLOR PHOTOGRAPH

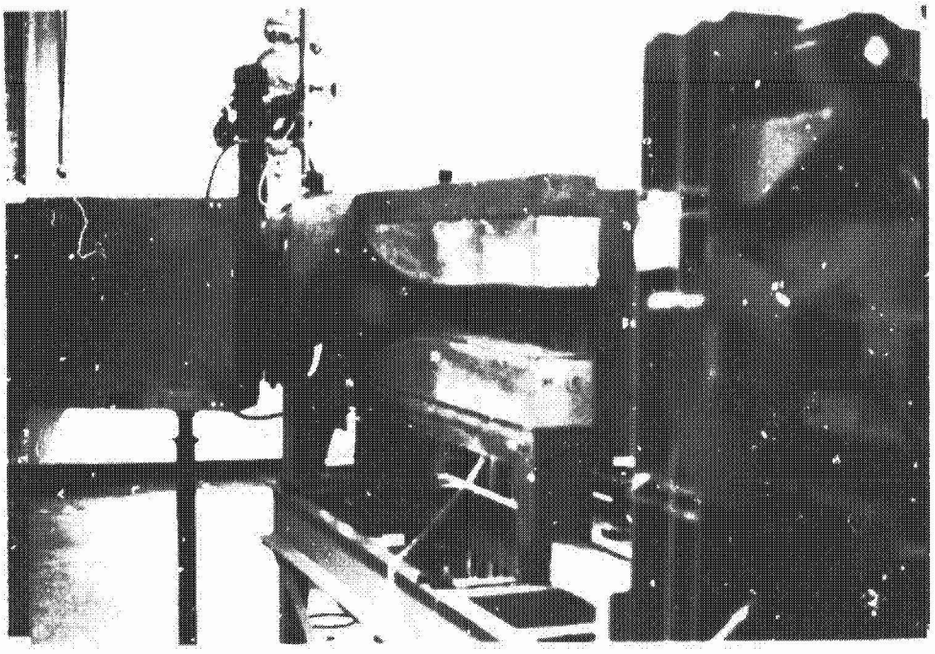

(a) Test Section with M-1.5 Nozzle Blocks

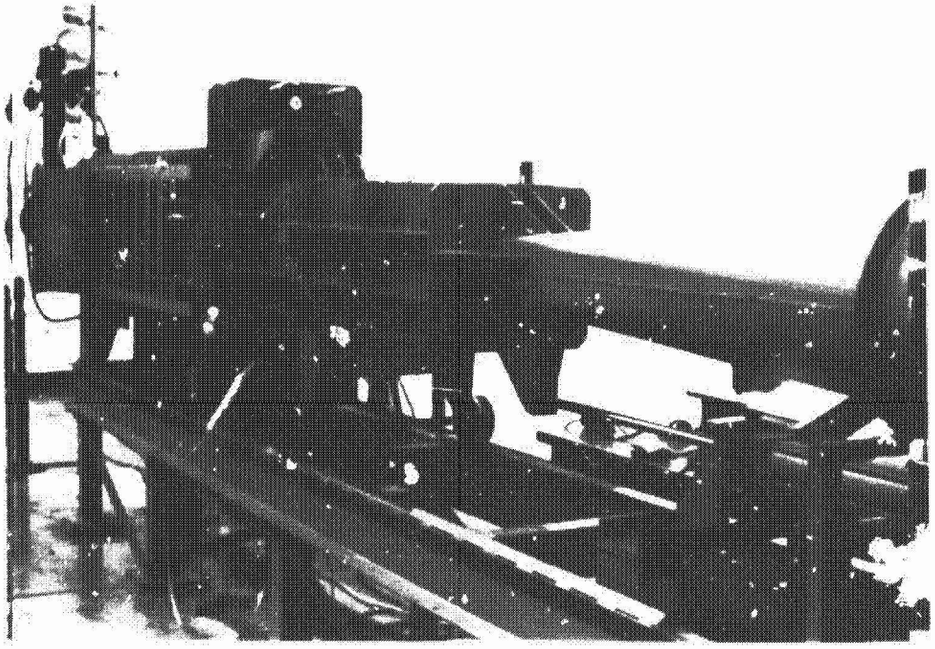

(b) Test Section and Diffuser

FIGURE 5. San Jose State University
High Speed Wind Tunnel

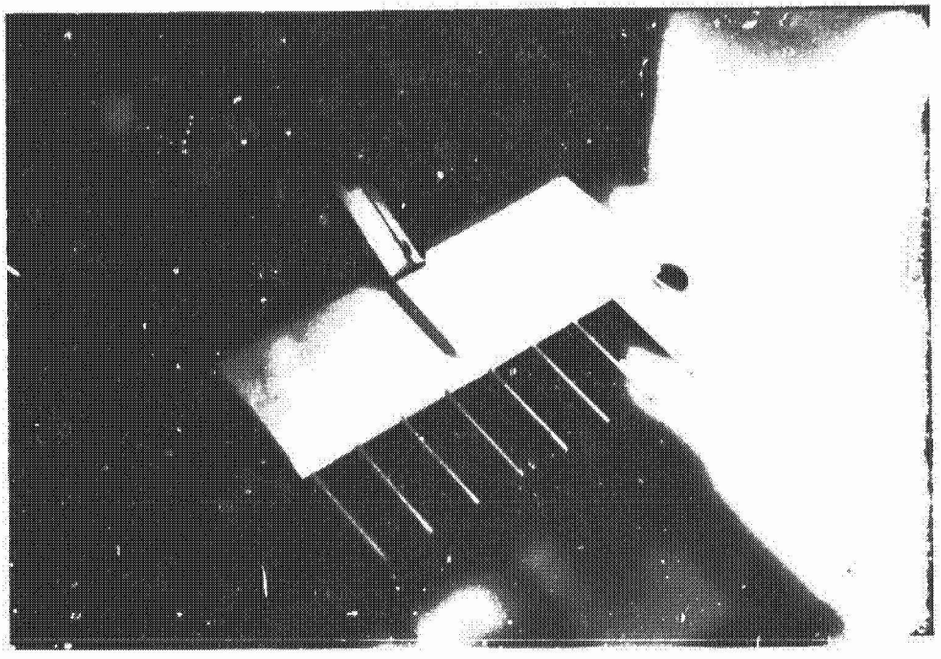

FIGURE 6. New Designed 9 Probe Rake

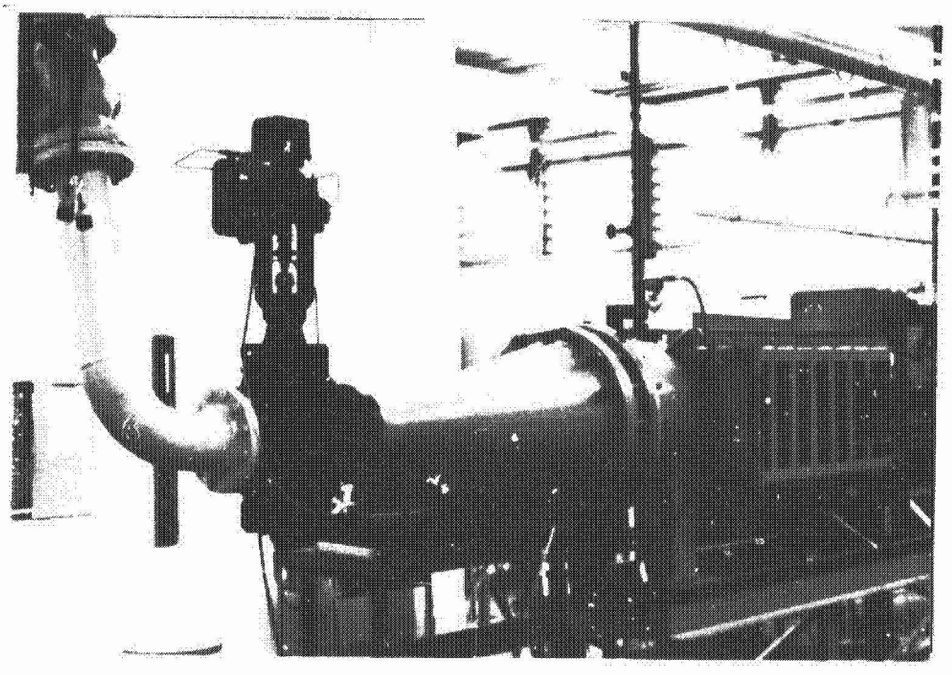

FIGURE 7. Pneumatic Controller & Valve Positioner for High Speed Tunnel

ORIGINAL PAGE
COLOR PHOTOGRAPH

FIGURE 8. One Half Inch Diameter Cone
Showing a 45° Mach Angle
With M-1.5 Nozzle Blocks

Fig. 9. Static Pressure Distribution for a Subsonic Run with Mach 1.5 Nozzle Blocks, Straight Channel Model, and Second Throat Area 6 x 2 3/4 Inches

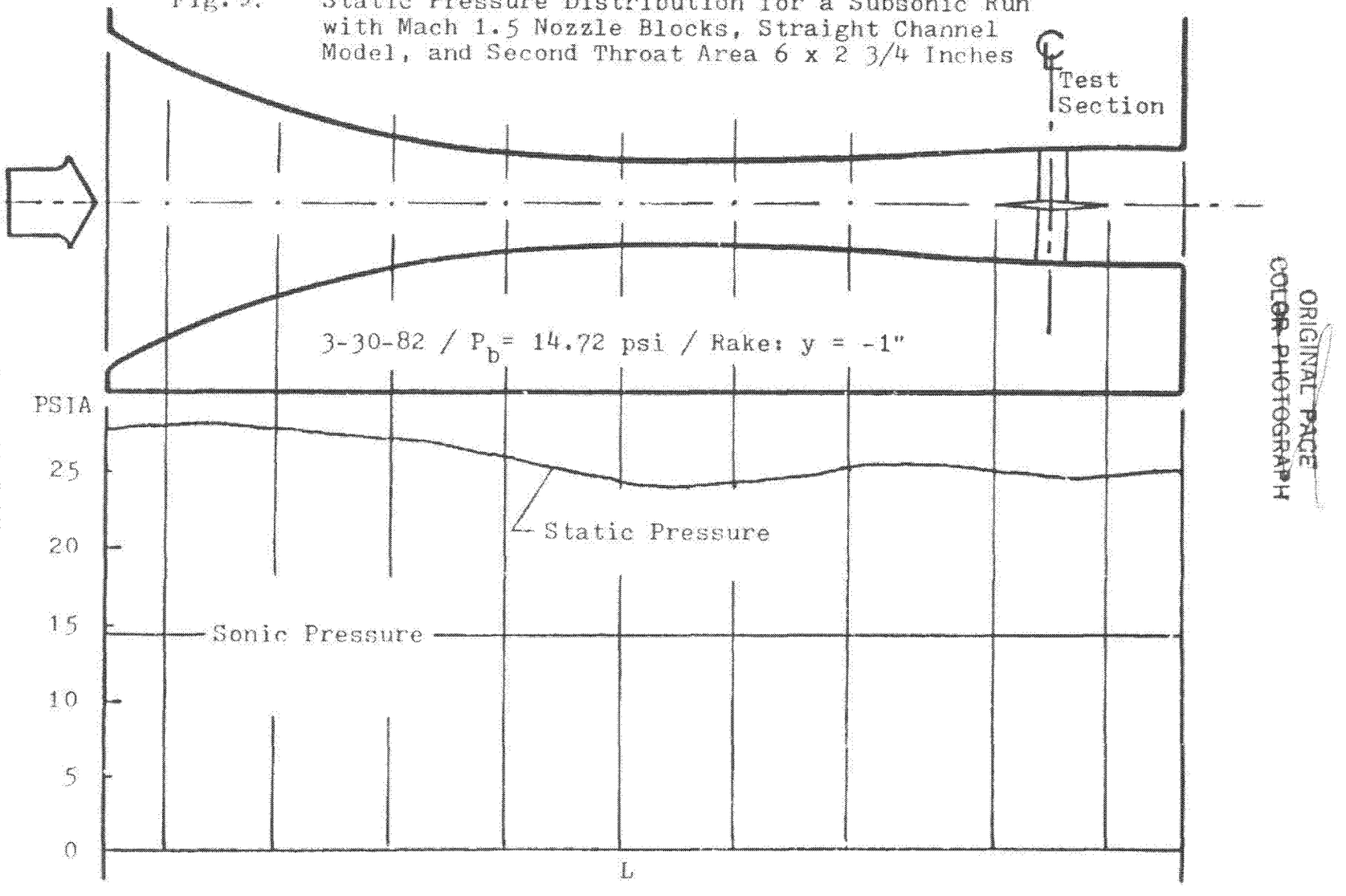

Fig. 10. Static Pressure Distribution for a Transonic Run with Mach 1.5 Nozzle Blocks, Straight Channel Model, and Second Throat Area 6 x 6 Inches

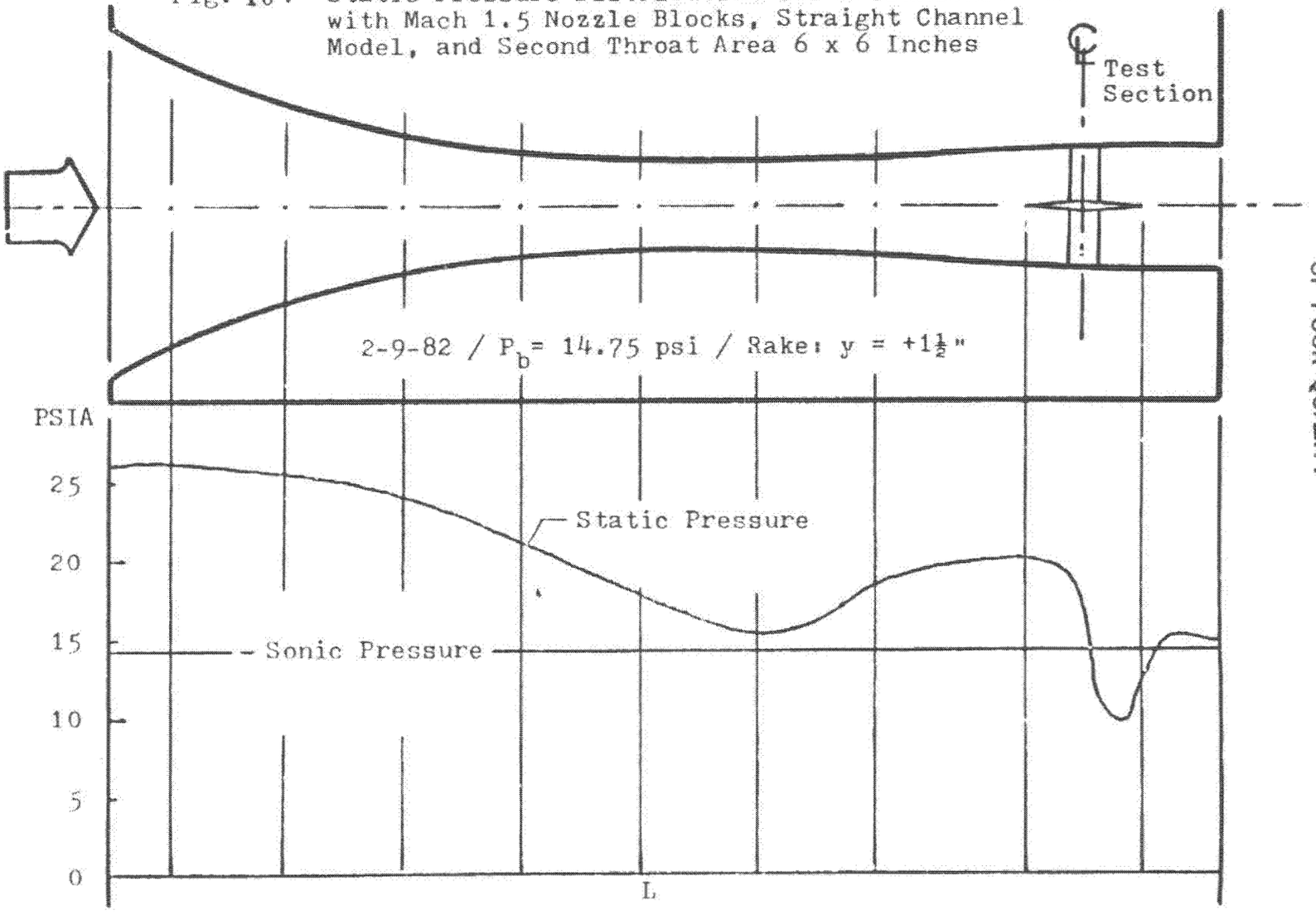

Fig. 11. Static Pressure Distribution for a Transonic Run with Mach 1.5 Nozzle Blocks, Area Ruled Channel Model, and Second Throat Area 6 x 6 Inches

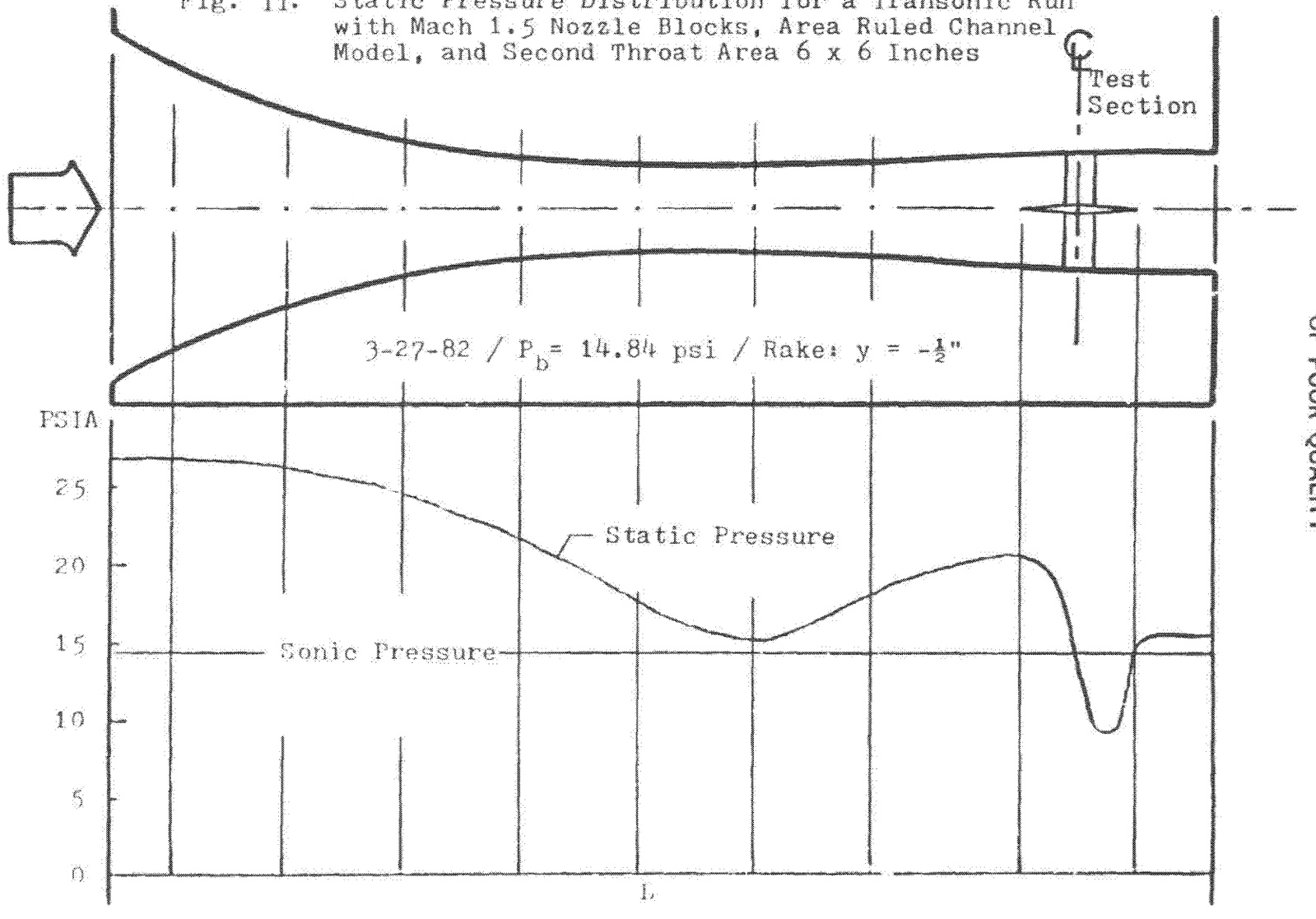

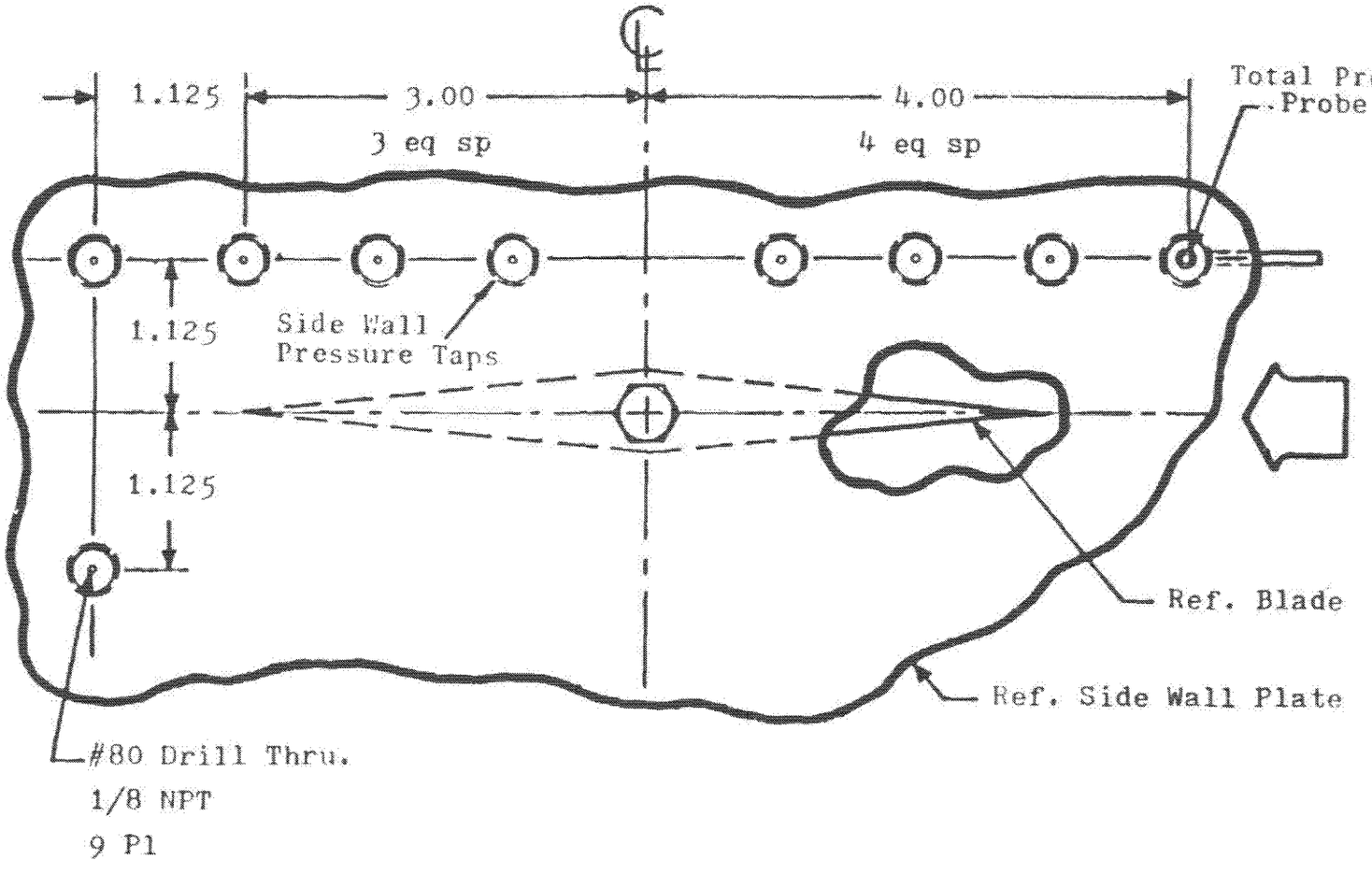

Fig. 12. Modified Left Hand Side Wall Plate with Pressure Taps

Fig. 13. Static Pressure Distribution for a Supersonic Run with Mach 2 Nozzle Blocks, Straight Channel Model, and Second Throat Area 6 x 6 Inches

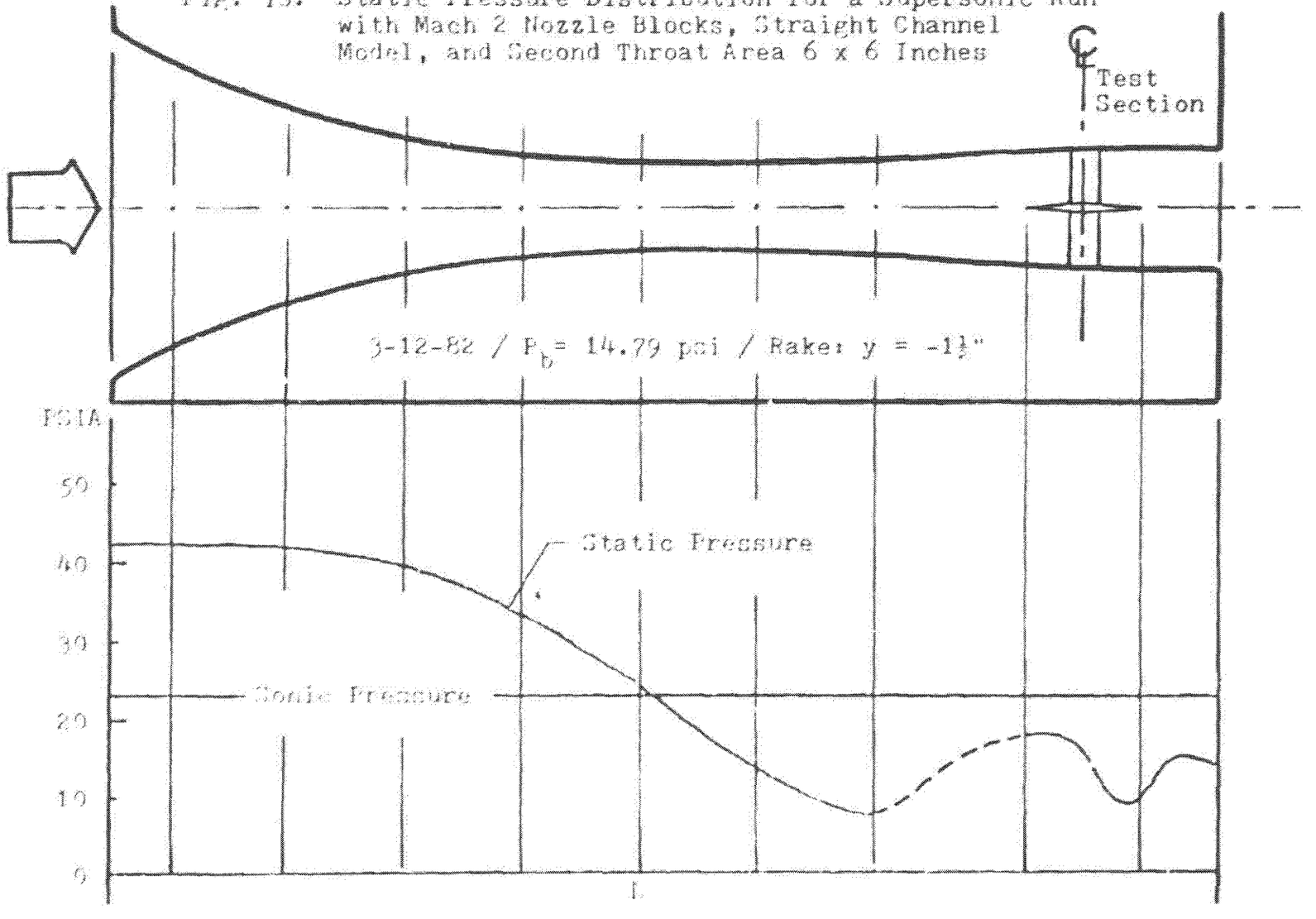

Fig. 14. Static Pressure Distribution for a Supersonic Run with Mach 2 Nozzle Blocks, Area Ruled Channel Model, and Second Throat Area 6 x 6 Inches

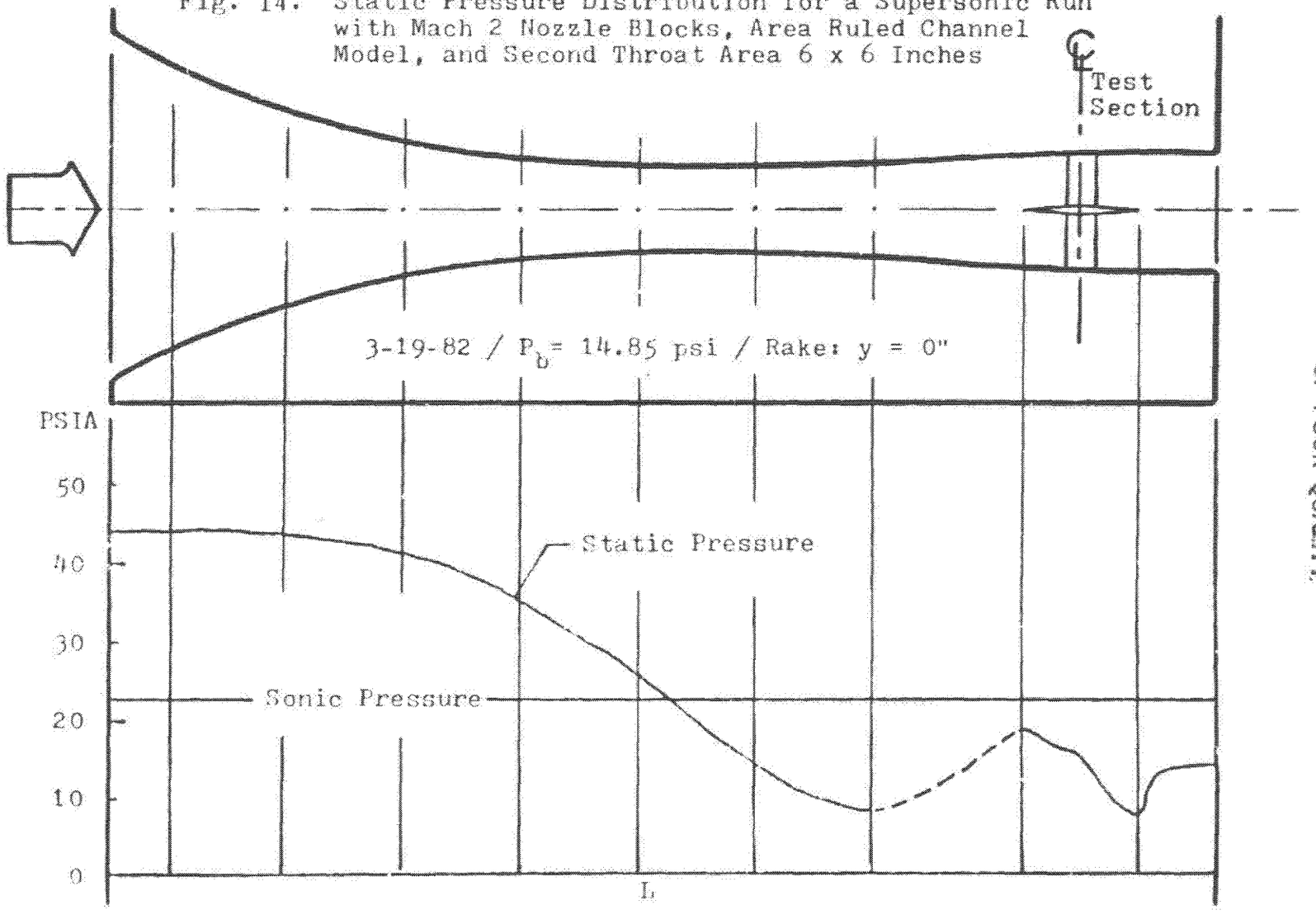

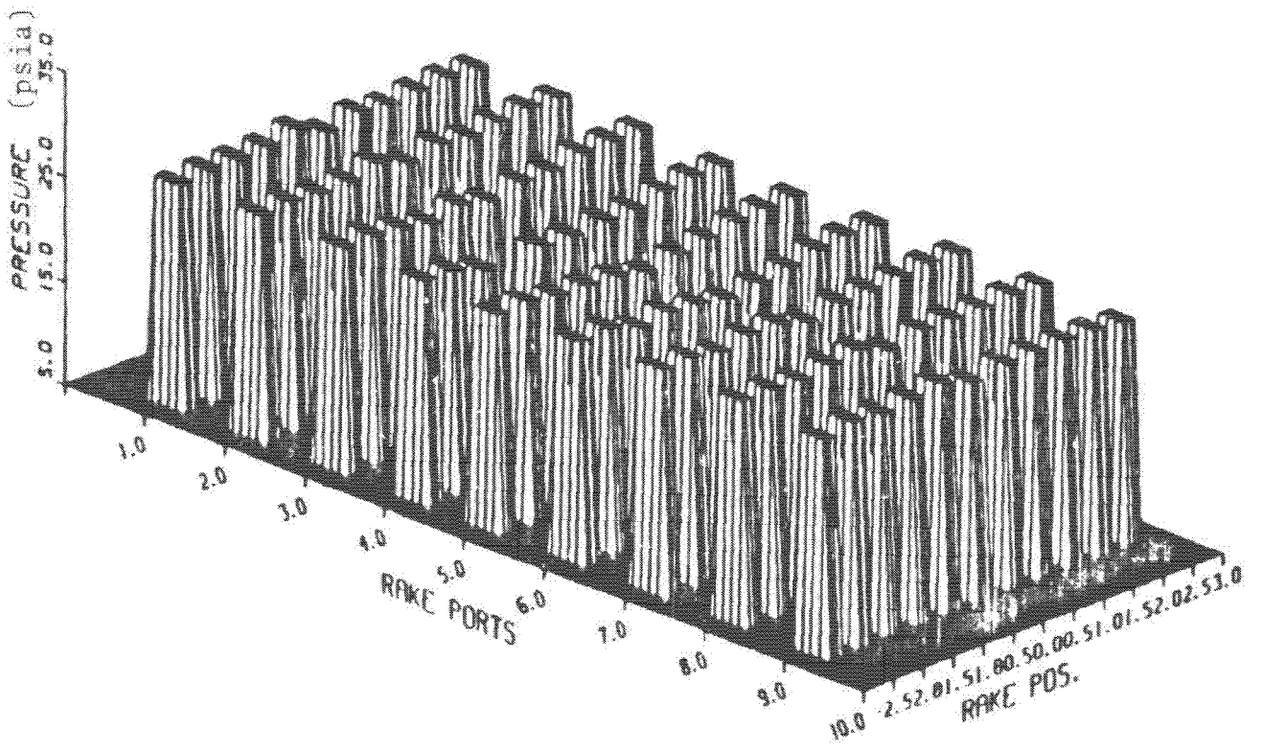

Fig. 15. Pressure Profile of Subsonic Runs with Mach 1.5 Nozzle Blocks and Straight Channel Model

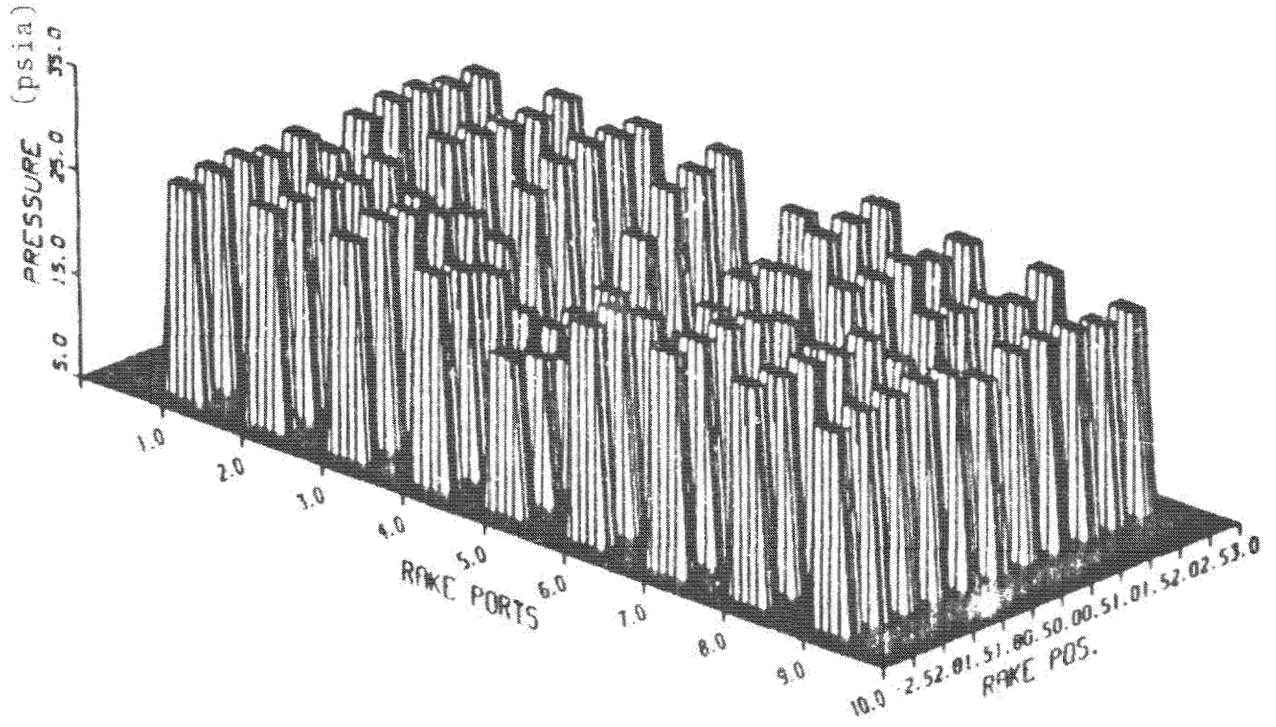

Fig. 16. Pressure Profile of Transonic Runs with Mach 1.5 Nozzle Blocks and Straight Channel Model

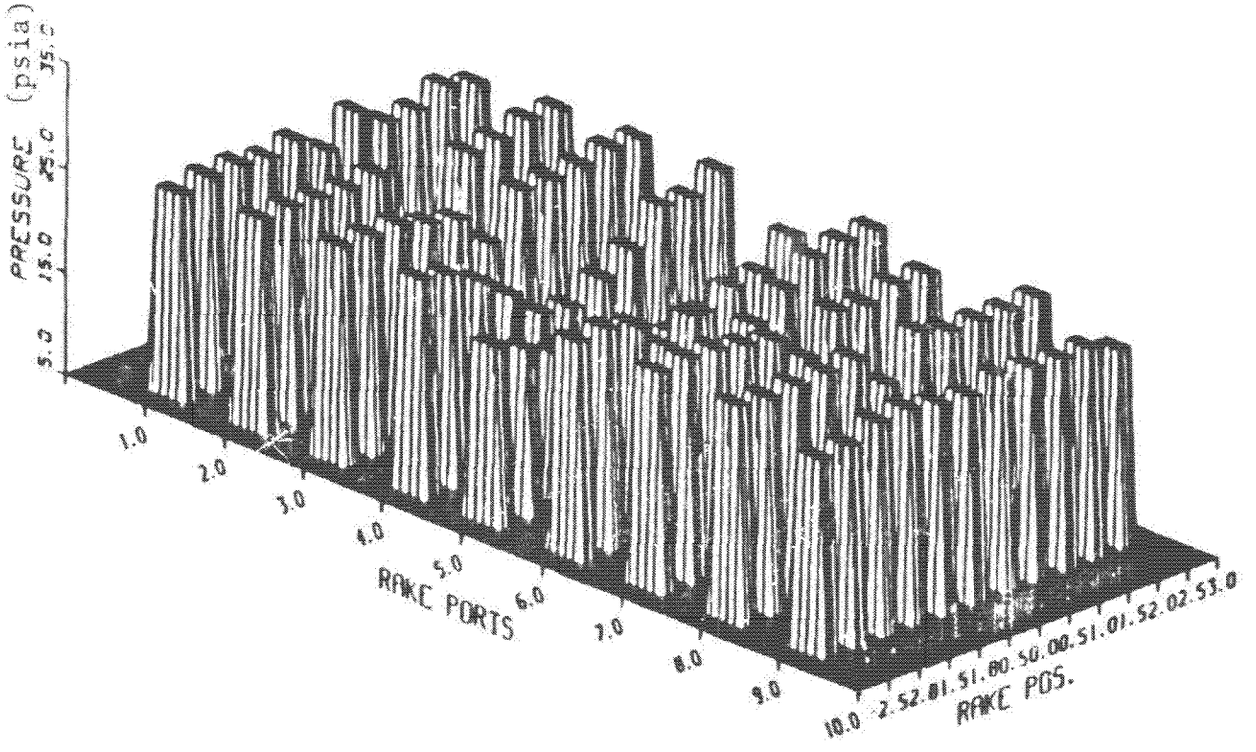

Fig. 17. Pressure Profile of Transonic Runs with Mach 1.5 Nozzle Blocks and Area Ruled Channel Model

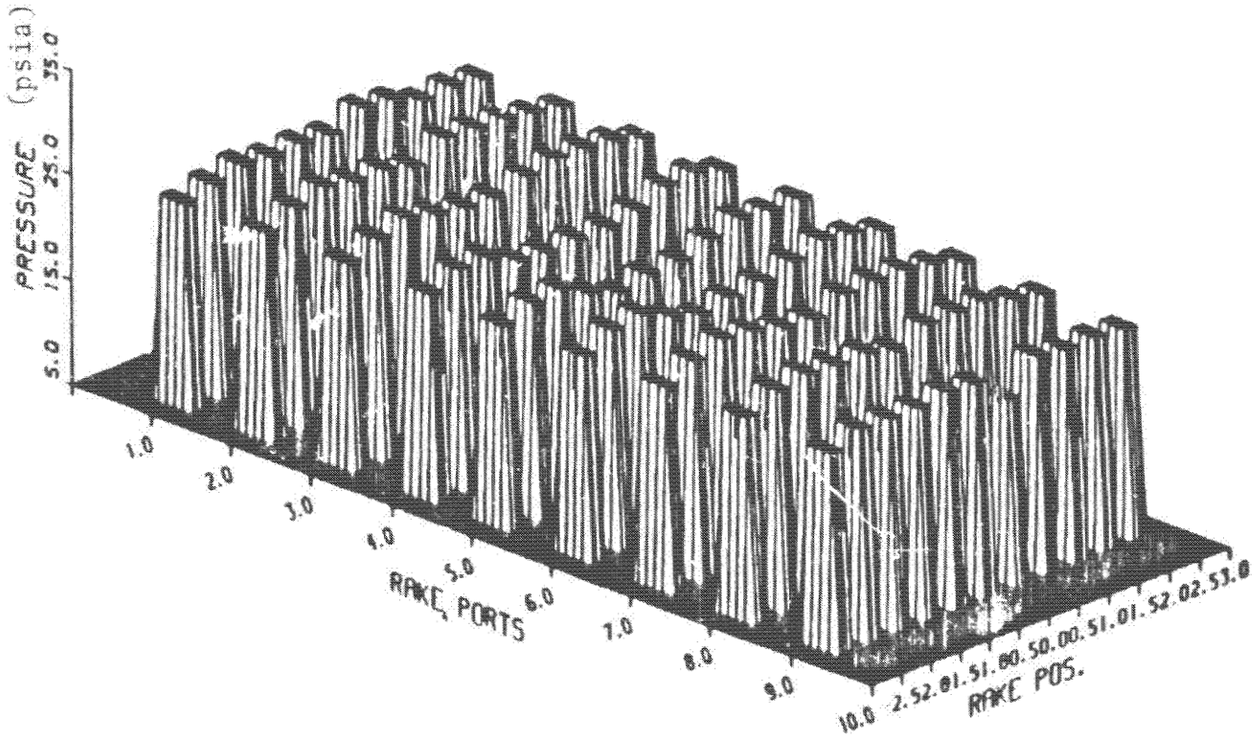

Fig. 18 . Pressure Profile of Subsonic Runs with Mach 2 Nozzle Blocks and Straight Channel Model

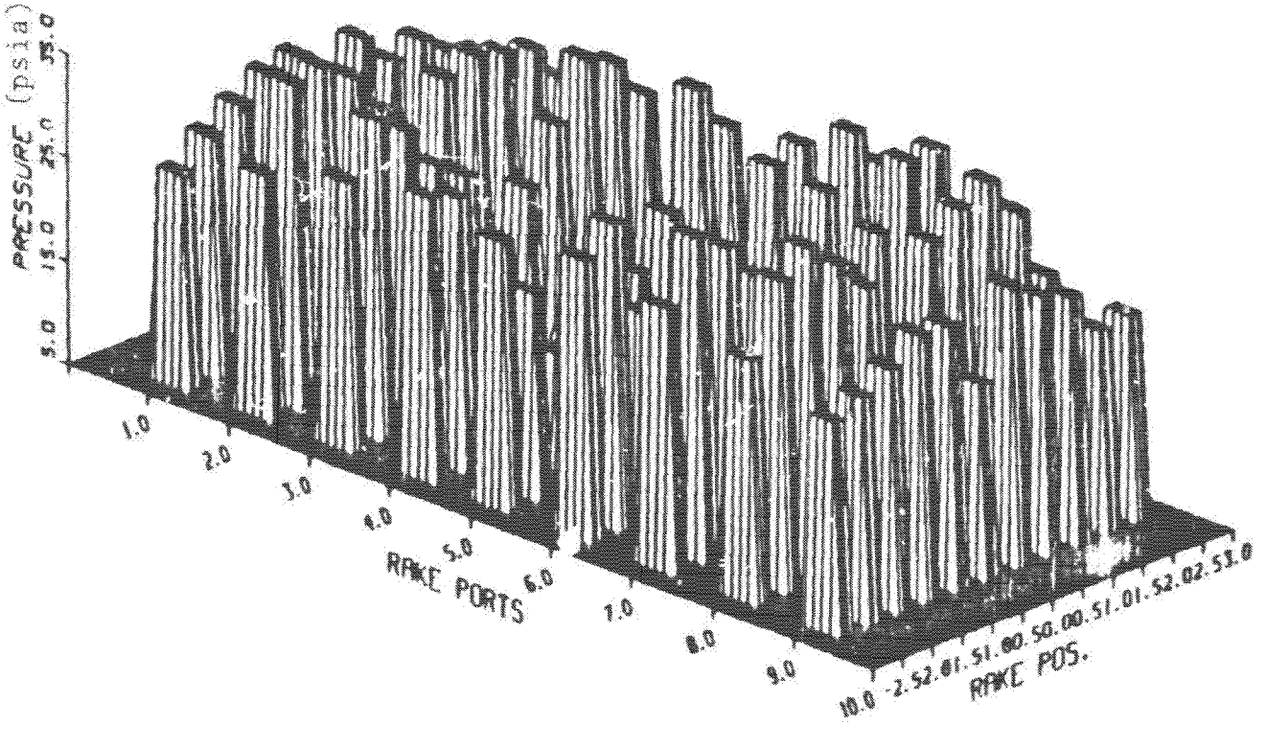

Fig. 19. Pressure Profile of Supersonic Runs with Mach 2 Nozzle Blocks and Straight Channel Model

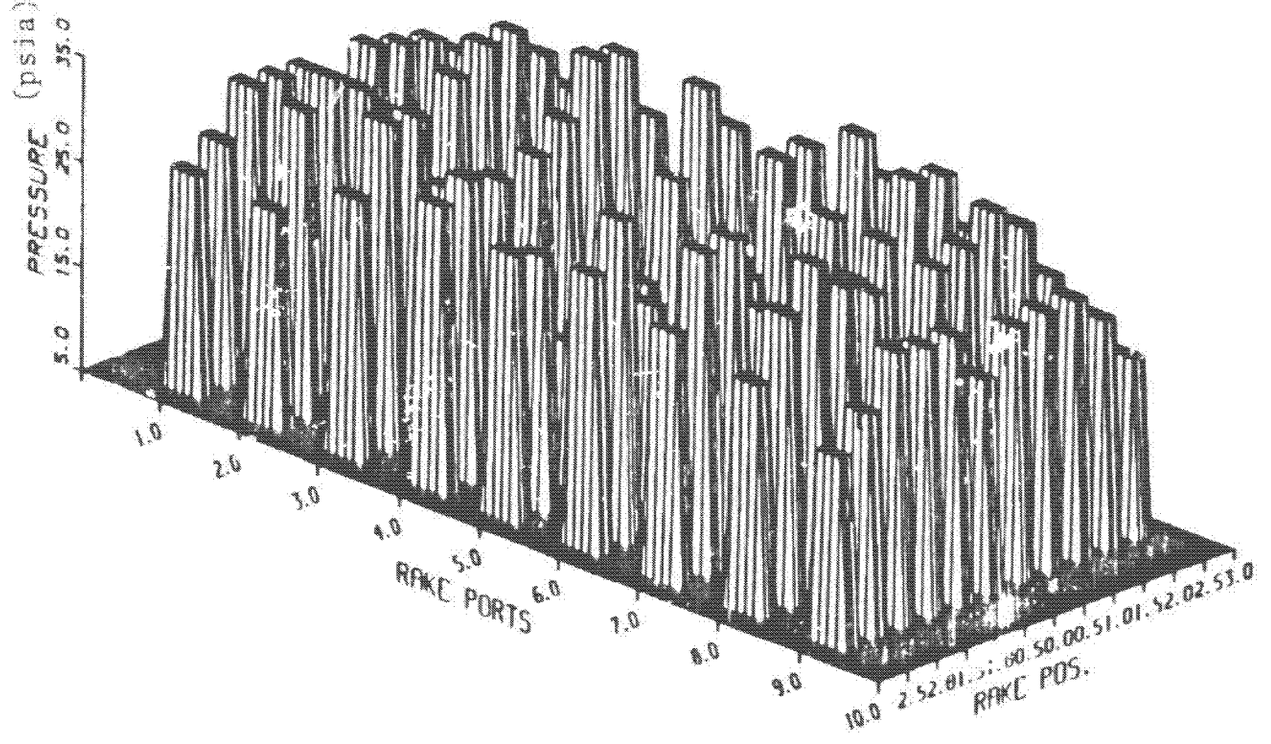

Fig. 20. Pressure Profile of Supersonic Runs with Mach 2 Nozzle Blocks and Area Ruled Channel Model

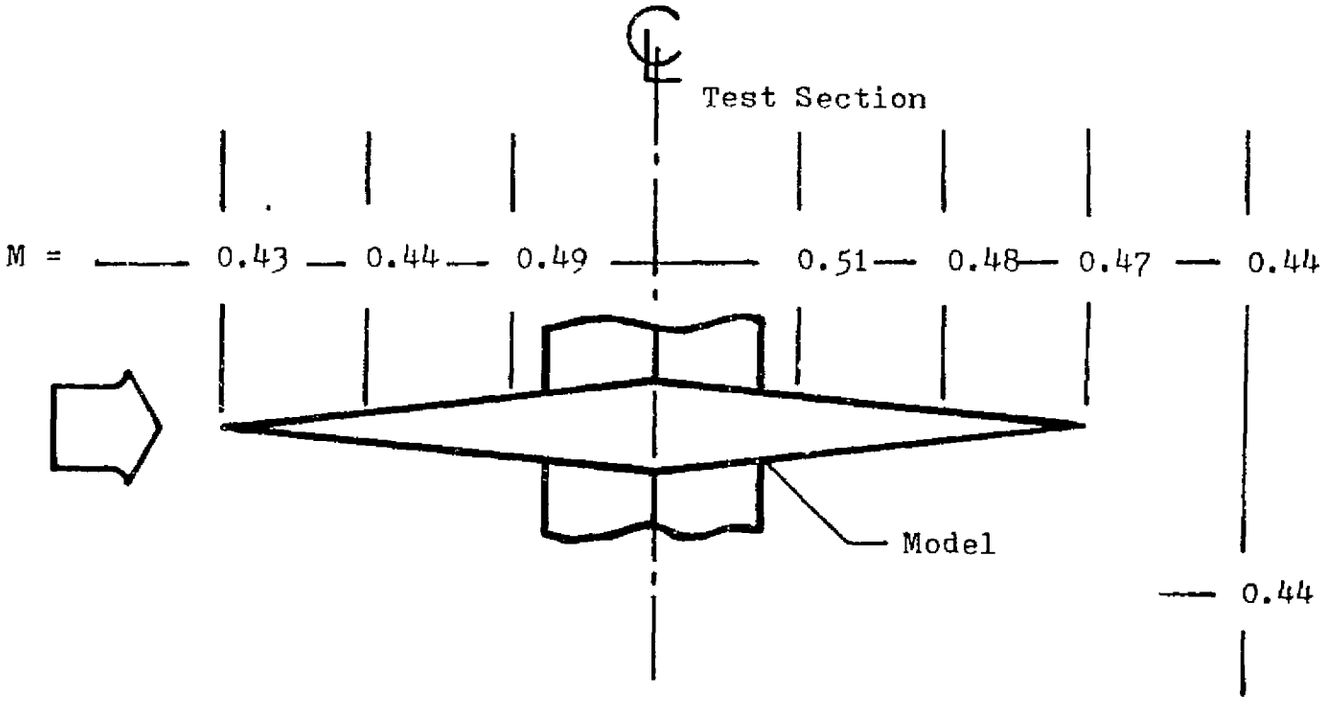

Fig. 21. Average Mach Numbers at Locations Relative to Model for Subsonic Runs with Mach 1.5 Nozzle Blocks and Straight Model Configuration

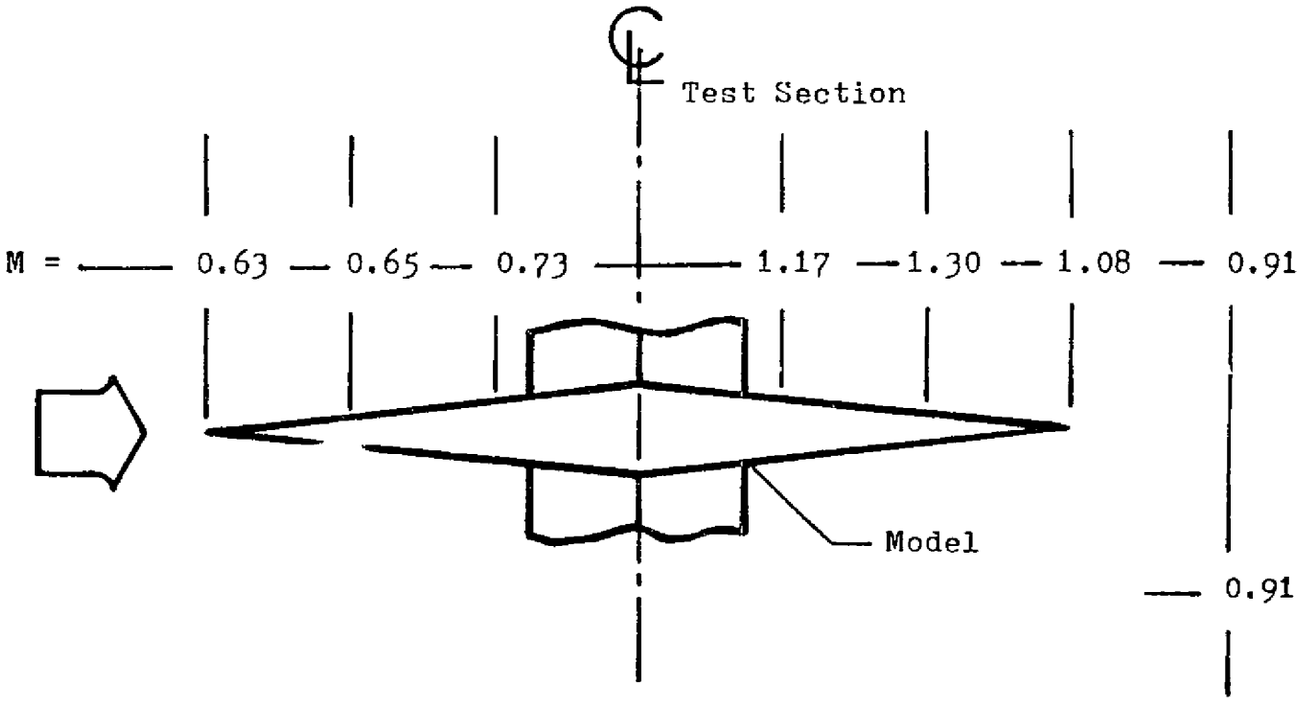

Fig. 22. Average Mach Numbers At Locations Relative to Model for Transonic Runs with Mach 1.5 Nozzle Blocks and Straight Model Configuration

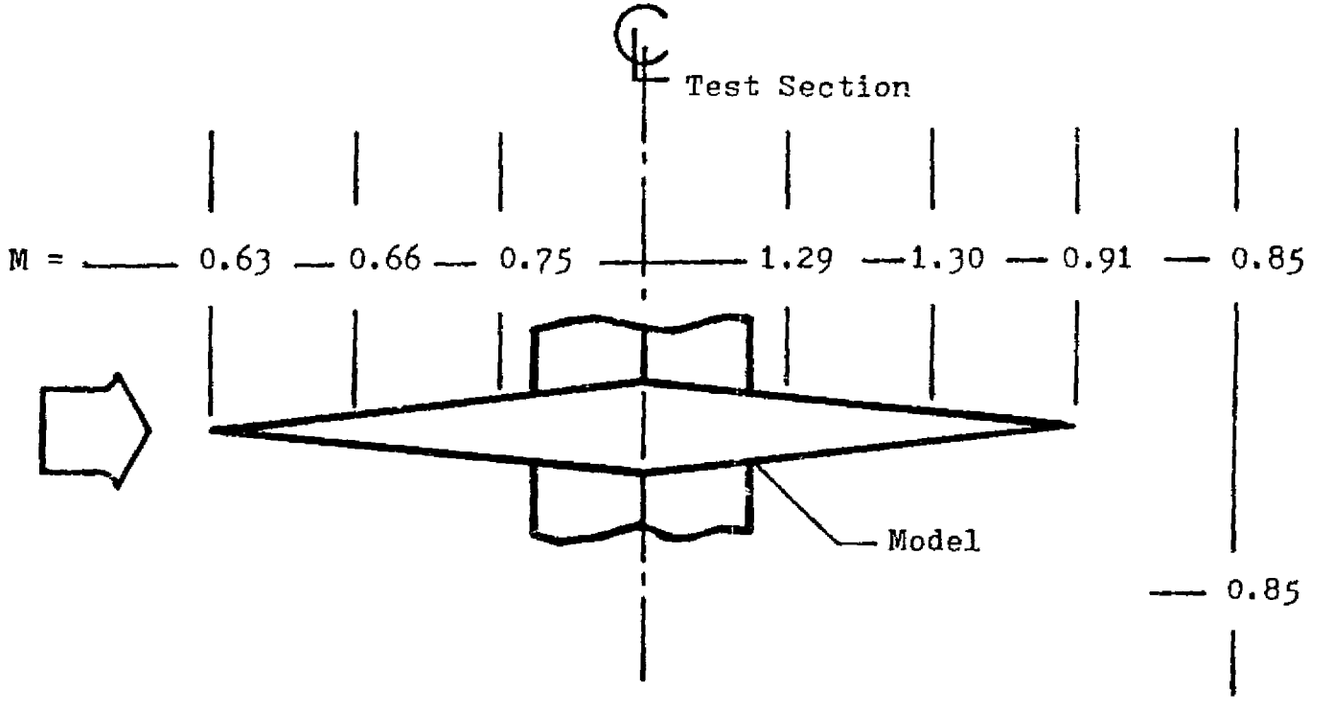

Fig. 23. Average Mach Numbers At Locations Relative to Model for Transonic Runs with Mach 1.5 Nozzle Blocks and Area Ruled Model Configuration

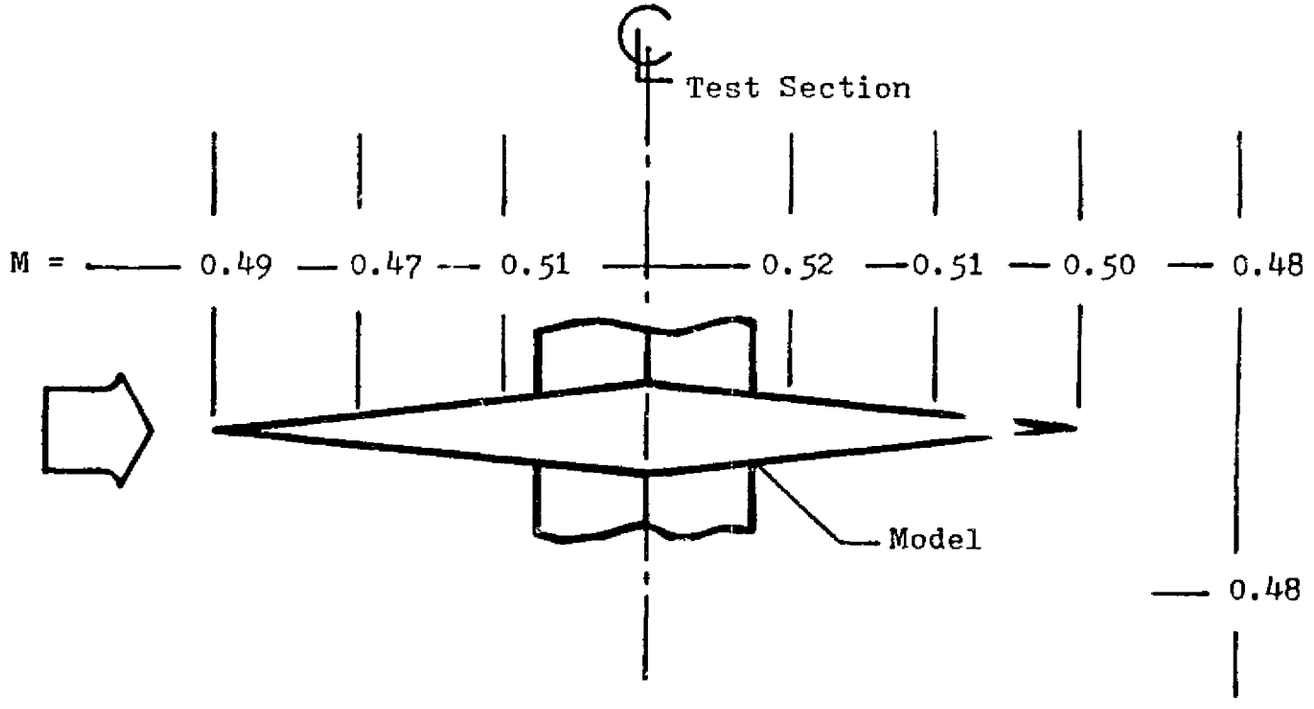

Fig. 24. Average Mach Numbers At Locations Relative to Model for Subsonic Runs with Mach 2 Nozzle Blocks and Straight Model Configuration

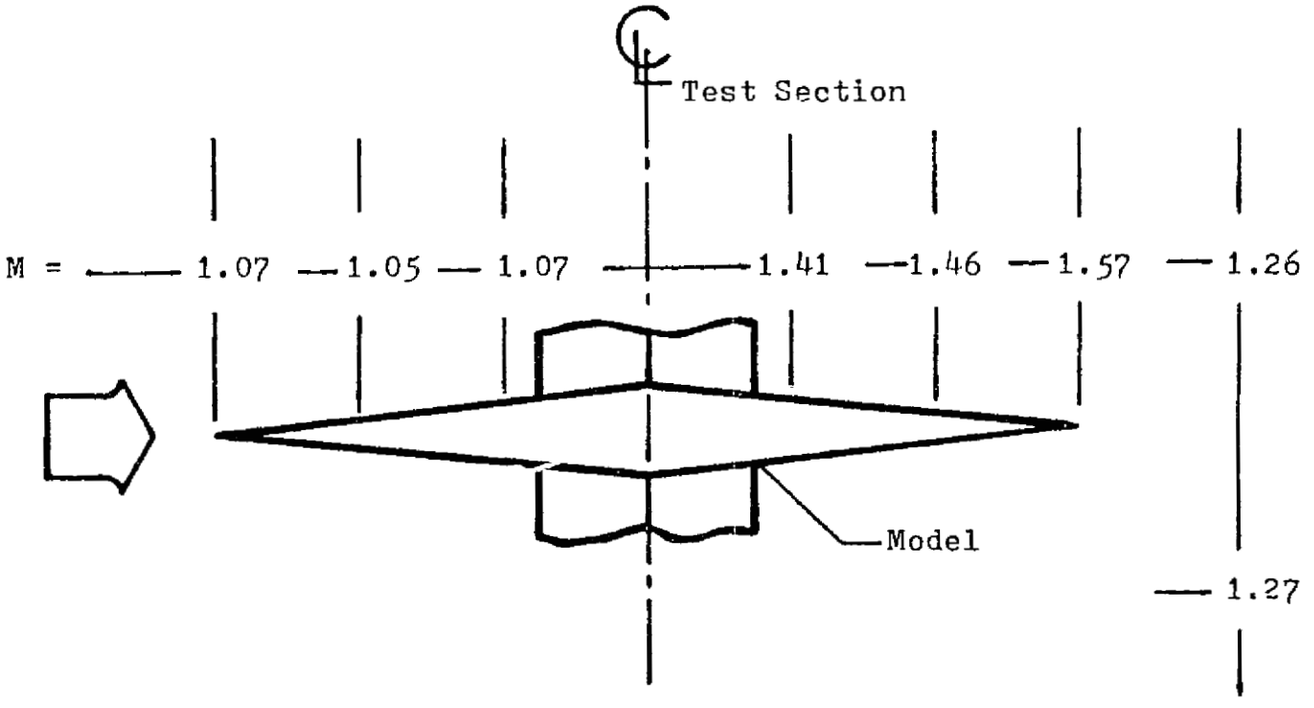

Fig. 25 . Average Mach Numbers At Locations Relative to Model for Supersonic Runs with Mach 2 Nozzle Blocks and Straight Model Configuration

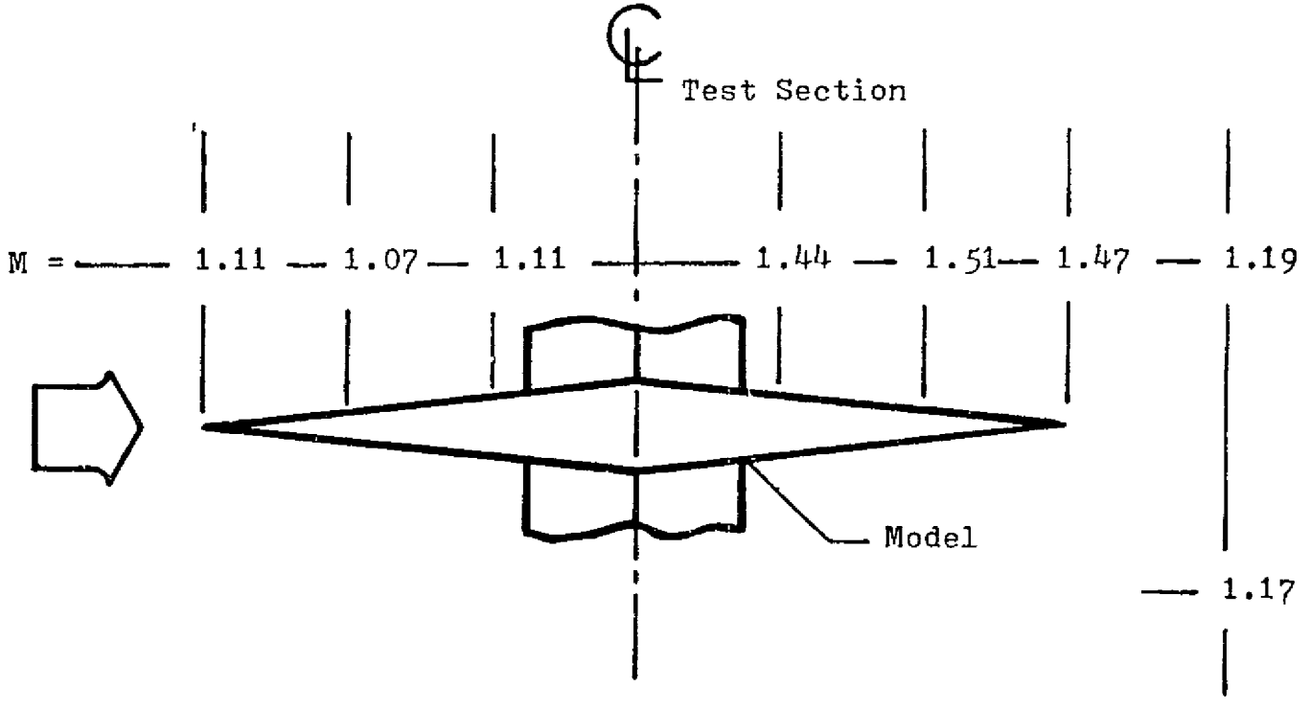

Fig. 26. Average Mach Numbers At Locations Relative to Model for Supersonic Runs with Mach 2 Nozzle Blocks and Area Ruled Model Configuration

ORIGINAL PAGE
COLOR PHOTOGRAPH

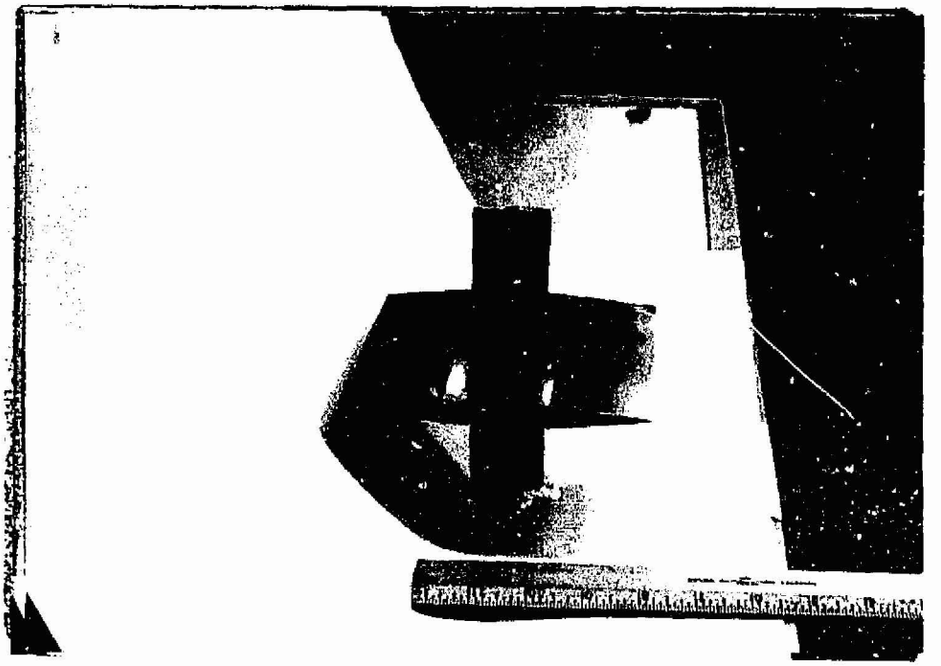

FIGURE 27. Double Trapezoid Blade and Damper Model

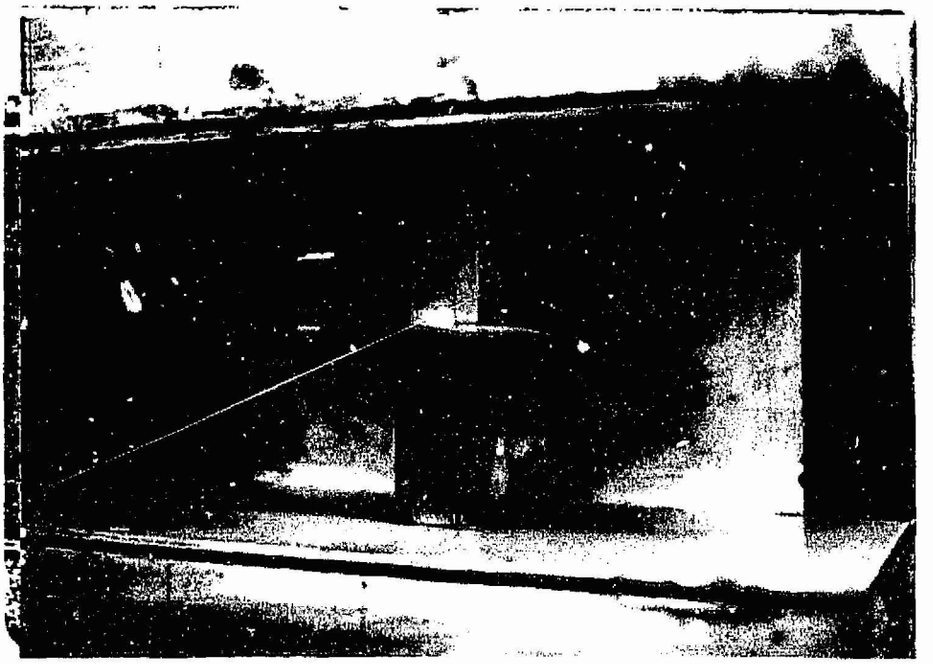

FIGURE 28. Double Trapezoid Model Installed with M = 1.5 Nozzle Blocks and Damper Area Ruling

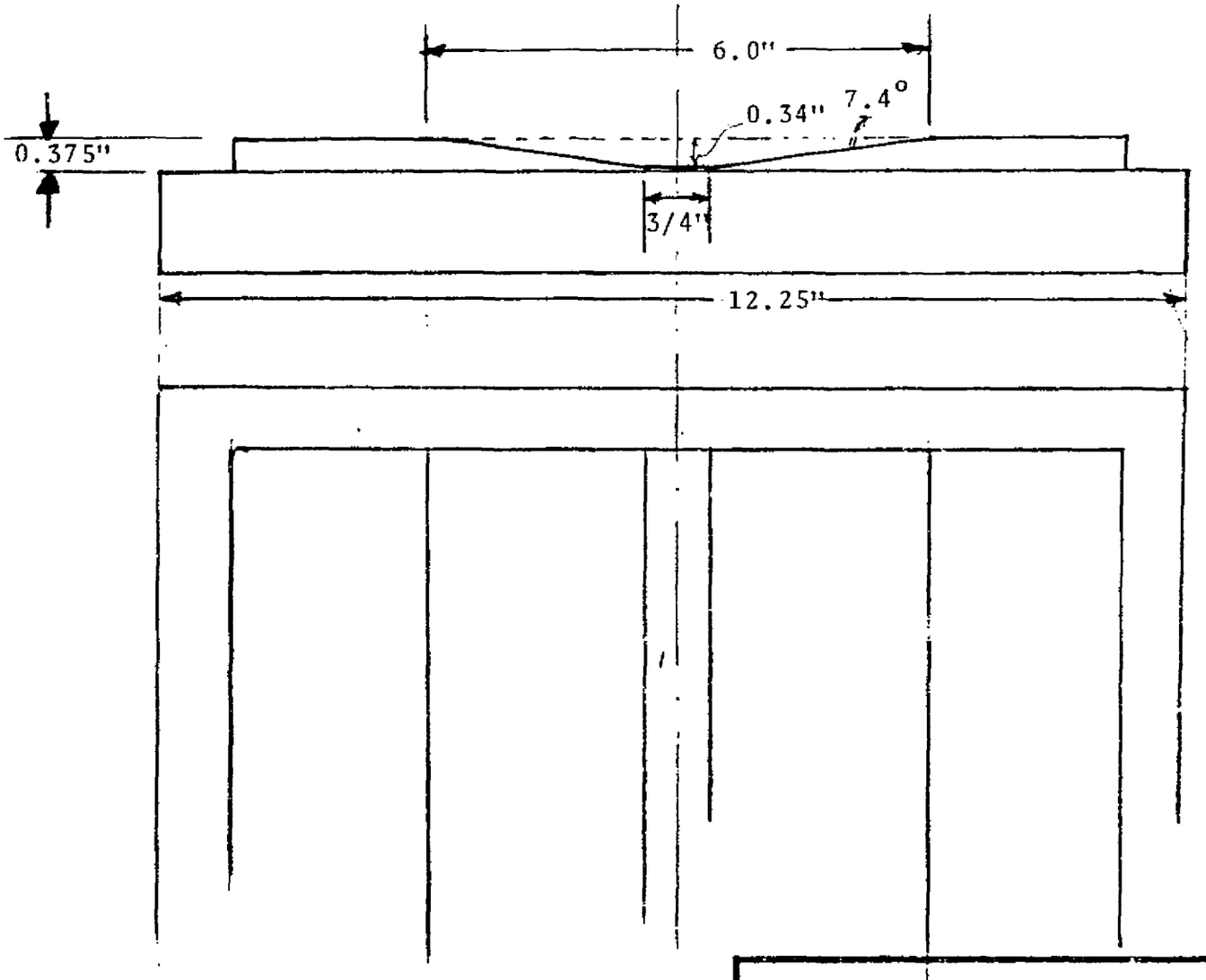

FIGURE 29

SIDE PLATES WITH DAMPER AND BLADE AREA RULING

SCALE: 1 : 2	APPROVED BY: W B Roberts	DRAWN BY: G R
DATE: 5/17/82		REVISED
		DRAWING NUMBER

FIGURE 30. Static Pressure Distributions for a Double Trapezoid Model with Mach 1.5 Nozzle Blocks and Second Throat Area 6 X 6 Inches

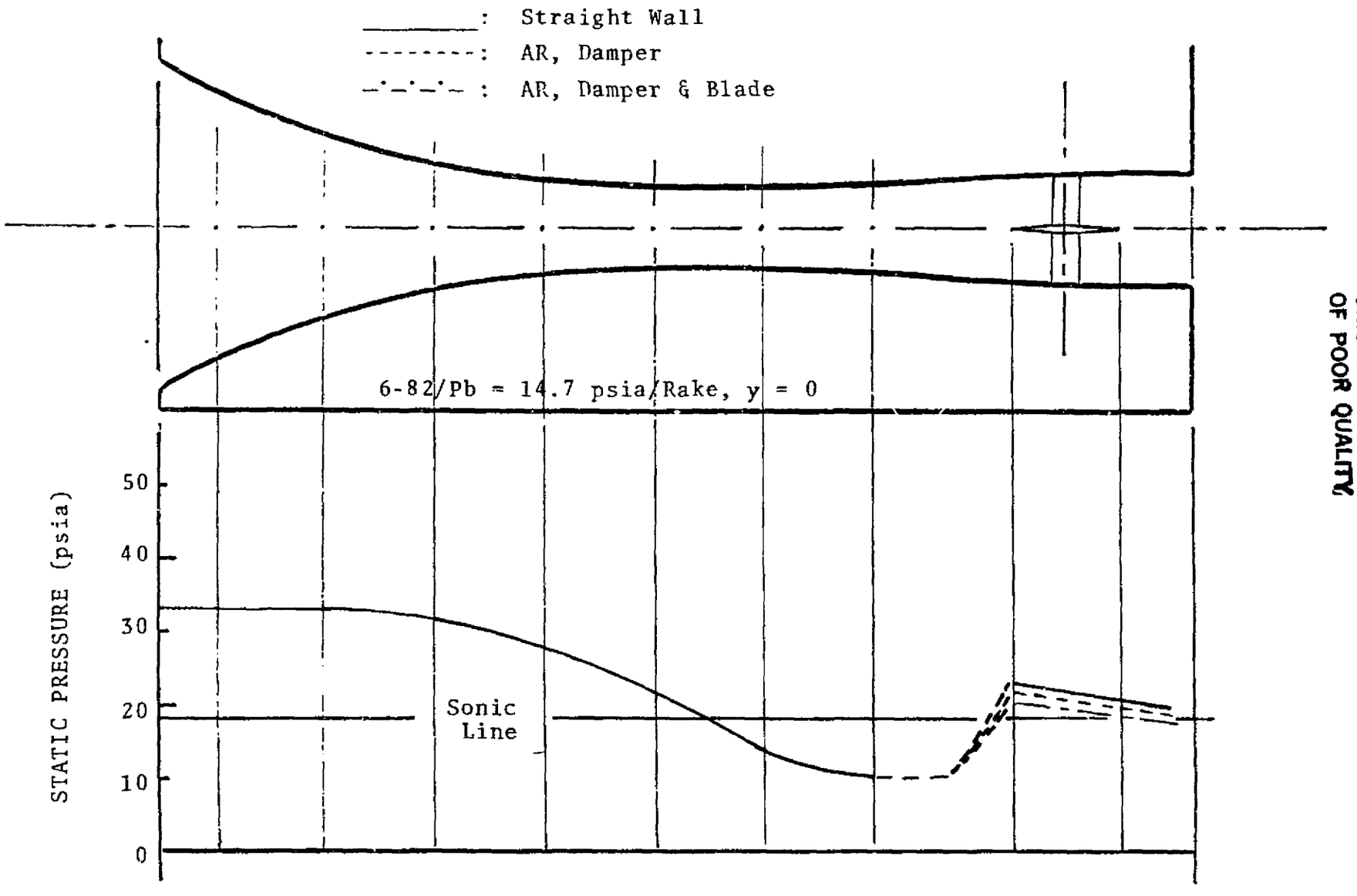

FIGURE 31. Static Pressure Distribution for a Double Trapezoid Model with Mach 2 Nozzle Blocks and Second Throat Area 6 X 6 Inches

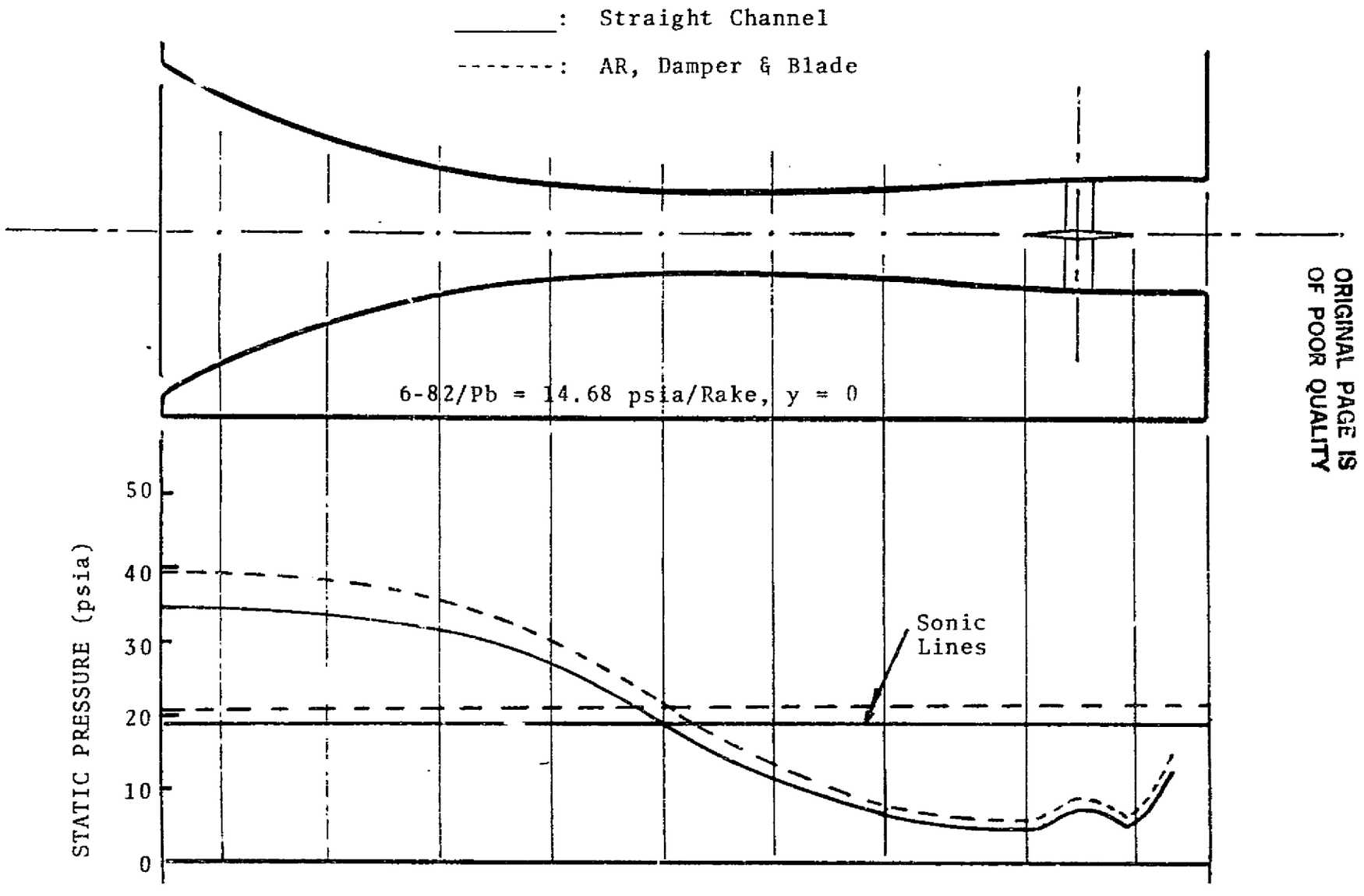

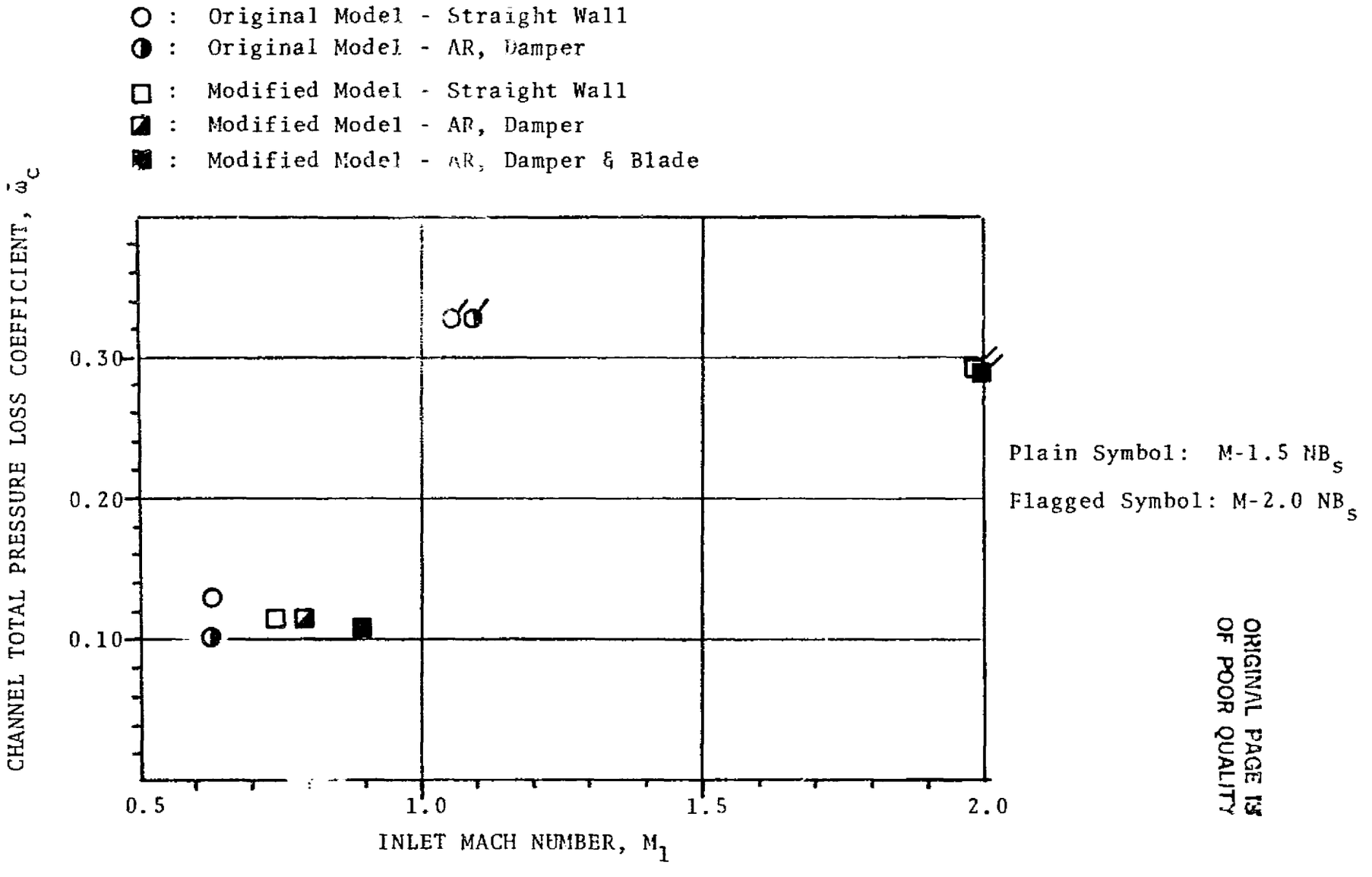

FIGURE 32 Total Pressure Loss Coefficient for Transonic and Supersonic Channel Flow